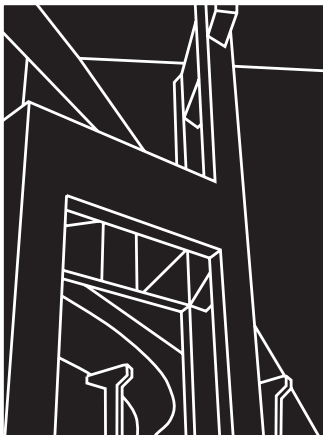


RESEARCH REPORT 987-8

COLLECTION AND ANALYSIS OF AUGMENTED WEIGH-IN-MOTION DATA

Clyde E. Lee and Joseph E. Garner



CENTER FOR TRANSPORTATION RESEARCH
BUREAU OF ENGINEERING RESEARCH
THE UNIVERSITY OF TEXAS AT AUSTIN

December 1996

1. Report No. TX-99/987-8		2. Government Accession No.		3. Recipient's Catalog No.	
4. Title and Subtitle COLLECTION AND ANALYSIS OF AUGMENTED WEIGH-IN-MOTION DATA				5. Report Date December 1996	
				6. Performing Organization Code	
7. Author(s) Clyde E. Lee and Joseph E. Garner				8. Performing Organization Report No. 987-8	
9. Performing Organization Name and Address Center for Transportation Research The University of Texas at Austin 3208 Red River, Suite 200 Austin, TX 78705-2650				10. Work Unit No. (TRAIS)	
				11. Contract or Grant No. Project 7-987	
12. Sponsoring Agency Name and Address Texas Department of Transportation Research and Technology Transfer Section/Construction Division P.O. Box 5080 Austin, TX 78763-5080				13. Type of Report and Period Covered Research Report (9/95-8/96)	
				14. Sponsoring Agency Code	
15. Supplementary Notes Project conducted in cooperation with the Texas Department of Transportation.					
16. Abstract <p>Traffic loading data are essential for the planning and design of adequate and cost-effective highway pavements. Data from an augmented weigh-in-motion (WIM) system have been collected and analyzed. The augmented WIM systems, which comprise bending-plate weighpads, infrared sensors, inductance loop detectors, and thermocouples, were installed in the southbound lanes of Highway 59 in east Texas in 1992. Data have been collected continuously since December 1992 for each vehicle and include date, time, lane, speed, number of axles, axle spacing, and wheel loads. The infrared sensors measure the lateral position of vehicle tires in the traffic lane and indicate single or dual tires. Hourly pavement and air temperatures are recorded by the thermocouples.</p> <p>While some preliminary data analysis is done on-site by the WIM-system computer, an Excel spreadsheet macro computer program was written for further data analysis, including vehicle classification and calculation of equivalent single axle loads (ESALs), a common way of expressing traffic loading. Some data trends have been analyzed, including the proportion of various vehicle classes and lane use. Periodic trends by day of the week and month of the year have also been examined.</p> <p>A methodology is outlined and illustrated for using traffic-volume and vehicle-class data, which are more commonly available than axle-load data, to estimate ESALs. The average ESAL factor per axle group of a given vehicle class is used to convert vehicles per day to ESALs per day. The cumulative ESALs at a site depend on the traffic volume and axle loads and may vary by the day of the week and season of the year. A growth-rate factor may be applied to forecast ESAL totals for future periods of time. Total predicted ESALs are used in the design and analysis of pavement structures.</p>					
17. Key Words Weigh-in-motion systems, pavement rehabilitation, Lufkin District, US 59, overlay strategies, traffic loads			18. Distribution Statement No restrictions. This document is available to the public through the National Technical Information Service, Springfield, Virginia 22161.		
19. Security Classif. (of report) Unclassified		20. Security Classif. (of this page) Unclassified		21. No. of pages 104	22. Price

**COLLECTION AND ANALYSIS OF AUGMENTED
WEIGH-IN-MOTION (WIM) DATA**

by

Clyde E. Lee
Joseph E. Garner

Research Report Number 987-8

Research Project 7-987

Project Title: *A Long-Range Plan for the Rehabilitation of US 59 in the Lufkin District*

Conducted for the

TEXAS DEPARTMENT OF TRANSPORTATION

by the

**CENTER FOR TRANSPORTATION RESEARCH
Bureau of Engineering Research
THE UNIVERSITY OF TEXAS AT AUSTIN**

December 1996

ABSTRACT

Traffic loading data are essential for the planning and design of adequate and cost-effective highway pavements. Data from an augmented weigh-in-motion (WIM) system have been collected and analyzed. The augmented WIM systems, which comprise bending-plate weighpads, infrared sensors, inductance loop detectors, and thermocouples, were installed in the southbound lanes of Highway 59 in east Texas in 1992. Data have been collected continuously since December 1992 for each vehicle and include date, time, lane, speed, number of axles, axle spacing, and wheel loads. The infrared sensors measure the lateral position of vehicle tires in the traffic lane and indicate single or dual tires. Hourly pavement and air temperatures are recorded by the thermocouples.

While some preliminary data analysis is done on-site by the WIM-system computer, an Excel spreadsheet macro computer program was written for further data analysis, including vehicle classification and calculation of equivalent single axle loads (ESALs), a common way of expressing traffic loading. Some data trends have been analyzed, including the proportion of various vehicle classes and lane use. Periodic trends by day of the week and month of the year have also been examined.

A methodology is outlined and illustrated for using traffic-volume and vehicle-class data, which are more commonly available than axle-load data, to estimate ESALs. The average ESAL factor per axle group of a given vehicle class is used to convert vehicles per day to ESALs per day. The cumulative ESALs at a site depend on the traffic volume and axle loads and may vary by the day of the week and season of the year. A growth-rate factor may be applied to forecast ESAL totals for future periods of time. Total predicted ESALs are used in the design and analysis of pavement structures.

ACKNOWLEDGMENTS

Throughout this research project a number of individuals provided information, suggestions, and assistance. Eric Starnater (LFK), an engineer in the Lufkin District of the Texas Department of Transportation, provided much assistance during and between field visits. Harry Thompson (LFK), the Area Engineer in Livingston, also provided project leadership and assistance. Willard Peavy and a crew from the Transportation Planning and Programming (TP&P) Division installed the weigh-in-motion system. Brian St. John from the TP&P Division assisted with the calibration of the weighpads. Siegfried Gassner from PAT Traffic Control Corporation provided assistance in setting up the software. James Stewart at The University of Texas at Austin manufactured infrared sensor housings and other items in the Department of Civil Engineering machine shop. Liren Huang at The University of Texas at Austin provided invaluable electronic and software expertise. The contributions from these people are greatly appreciated.

IMPLEMENTATION RECOMMENDATION

Augmented weigh-in-motion (WIM) systems have provided traffic loading data that are being used in the development of a long-range rehabilitation plan for pavements on US 59 within the Lufkin District. Bending-plate weighpads provided vehicle speed, class, and weight data. Infrared sensors provided information about the lateral position of vehicles within the lanes and indicated whether tires were single or dual. Thermocouples provided hourly air and pavement temperatures. A method has been outlined which can be used to forecast equivalent single axle loads (ESALs) from traffic volume and classification data using representative WIM data. In terms of implementation, the researchers suggest that the data collection and analysis procedures described herein can be used in other locations throughout Texas.

Prepared in cooperation with the Texas Department of Transportation

DISCLAIMERS

The contents of this report reflect the views of the authors, who are responsible for the facts and the accuracy of the data presented herein. The contents do not necessarily reflect the official views or policies of the Texas Department of Transportation. This report does not constitute a standard, specification, or regulation.

There was no invention or discovery conceived or first actually reduced to practice in the course of or under this contract, including any art, method, process, machine, manufacture, design or composition of matter, or any new and useful improvement thereof, or any variety of plant, which is or may be patentable under the patent laws of the United States of America or any foreign country.

NOT INTENDED FOR CONSTRUCTION, BIDDING, OR PERMIT PURPOSES

Clyde E. Lee, P.E. (Texas No. 20512)
Research Supervisor

TABLE OF CONTENTS

CHAPTER 1. INTRODUCTION	1
CHAPTER 2. BACKGROUND	3
2.1 Causes of Pavement Damage	3
2.1.1 AASHO Road Test.....	3
2.1.2 Other Factors	4
2.2 Traffic Data Collection.....	5
2.2.1 Weigh-in-Motion.....	5
2.2.2 Inductance Loop Detectors.....	7
2.2.3 Infrared Sensors.....	7
CHAPTER 3. EQUIPMENT INSTALLATION AND MAINTENANCE.....	11
3.1 U.S. 59 Rehabilitation Plan.....	11
3.1.1 Test Sections	11
3.1.2 Traffic and Temperature Monitoring	13
3.1.3 Pavement Monitoring.....	13
3.2 Test Section Construction and WIM Installation.....	15
3.3 Maintenance and Repair.....	21
3.3.1 Infrared Sensors.....	21
3.3.2 Modems and Software.....	22
CHAPTER 4. DATA ACQUISITION AND ANALYSIS	25
4.1 Preliminary Calculations	25
4.1.1 Speed and Spacing	25
4.1.2 Lateral Position and Dual Tires.....	27
4.1.3 Real-time Display.....	27
4.2 Calibration.....	28
4.2.1 Weight	28
4.2.2 Pavement Roughness.....	29
4.2.3 Lateral Position	29
4.2.4 Temperature	30

4.3 File Management and Sorting	30
4.3.1 Data Downloading.....	30
4.3.2 Excel Macros.....	31
CHAPTER 5. VOLUME AND SPEED.....	35
5.1 Vehicle Classification	35
5.2 Periodic Trends	39
CHAPTER 6. AXLE LOADS AND ESALS.....	47
6.1 Equivalent Single Axle Load Calculations	48
6.2 Periodic Trends	52
6.3 Prediction Algorithm.....	63
6.4 Summary	68
CHAPTER 7. LATERAL POSITION AND DUAL TIRES	69
7.1 Site and Lane Variation.....	69
7.2 Stripe Moving.....	73
7.3 Dual-Tire Data.....	74
CHAPTER 8. TEMPERATURE	81
8.1 Installation and Calibration	81
8.2 Daily and Seasonal Variations	82
CHAPTER 9. CONCLUSION.....	87
REFERENCES.....	91

SUMMARY

The primary cause of damage to highway pavements is traffic loading. The AASHO Road Test demonstrated that the damage caused by axle loads is nonlinear, with an approximate fourth-power relationship; thus, doubling the axle load results in multiplying the pavement damage by 16. Only uniform axle loads were applied at the Road Test, so the concept of the equivalent single axle load (ESAL) was introduced to describe the damage caused by mixed traffic loads in terms of a standard axle load. The number of applications of a standard single axle load of 8.2 Mg (18 kip) that would cause the same damage as one application of a given axle load is known as the ESAL factor.

Two pavement test sections were constructed in the southbound lanes of Highway 59 and augmented weigh-in-motion (WIM) systems were installed to measure traffic loads. The traffic data collected by the WIM systems include number of vehicles, wheel loads, speed, number of axles, axle spacing, lateral position, and indication of single or dual tires. The WIM systems were installed in 1992 and continuous data collection began in December 1992. Bending-plate weighpads sensed wheel load and other traffic data. Infrared sensors measured lateral position and dual tire data. Thermocouples provided air and pavement temperature.

Some preliminary data calculations were performed on-site, including weight, speed, and axle spacing for each vehicle. Modems were used to download data files over telephone lines. An Excel macro was used to sort vehicles into different files by vehicle class, to calculate ESALs and lateral position for each vehicle, and to summarize the data for each lane and vehicle class.

Volume, speed, axle load, and ESAL data trends were analyzed. An average of 7,000 vehicles passed each day in the southbound lanes. Right-lane vehicles accounted for 75 percent of the total volume and 88 percent of the total ESALs. Five-axle tractor semitrailer trucks (3S2 vehicles) accounted for approximately 15 percent of the right-lane volume and 80 percent of the right-lane ESALs. A method for estimating ESALs from traffic-volume and classification counts, using representative WIM data, is outlined. The lateral-position data showed that vehicles with more axles tended to travel closer to the shoulders than vehicles with fewer axles. The temperature data showed that the pavement temperature was almost always higher than the air temperature, except for a few hours in the mornings and on some days in the winter months.

This portion of Research Project 7-987 provided an opportunity for collecting and analyzing continuous, mixed-traffic data for correlation with concurrently measured performance of rigid and flexible pavement test sections. A unique weigh-in-motion system measured not only wheel loads, speed, and axle spacing, but also lateral position of tires, single or dual tires, and air and pavement temperatures. An Excel spreadsheet macro was written to display, arrange, and summarize a massive amount of data each day. Data were analyzed for one year to establish daily, weekly, and monthly patterns. Traffic loading data are essential in planning and designing adequate, cost-effective highway pavements.

Chapter 1 Introduction

Given that highway pavements represent an important part of our nation's infrastructure and, hence, have a significant impact on our economy, engineers are committed to addressing the ongoing issue of pavement damage. The majority of pavement damage is due to traffic loading, and in particular, to heavy trucks. Improving the performance of highway pavements would lead to a significant improvement in the cost of transportation, whether by reducing delay caused by maintenance and reconstruction or by decreasing the wear and tear on tires and vehicles. Traffic loading data have been collected and analyzed in this research project in order that the pavement designer may more efficiently allocate resources and minimize the effects of traffic loading.

This report is part of a series of reports describing the development of a long-range plan for the rehabilitation of Highway 59 pavements in the Lufkin District of the Texas Department of Transportation (TxDOT). The first reports discussed the development of the rehabilitation plan, the effect of work zone detours during construction, and the construction of the pavement test sections. Subsequent reports discussed the performance of the asphalt overlays and traffic load forecasting using weigh-in-motion (WIM) data. This report focuses on the installation of the augmented WIM systems and the collection and analysis of WIM data.

In Chapter 2, the AASHO Road Test, which led to the development of the equivalent single axle load (ESAL) concept, is described. Other factors, in addition to traffic loading, which contribute to pavement damage, are discussed. The backgrounds for the traffic data collection sensors used on this project are described. These sensors are WIM, inductance loop detectors, and infrared sensors.

The scope of Highway 59 Research Project 7-987 in east Texas is outlined in Chapter 3. The construction of two pavement test sections and the installation of the WIM systems are described. Infrared sensors are used to measure lateral position of tires and to indicate whether tires are single or dual. The solutions to some of the problems, which were experienced with the infrared sensors and modems, are discussed.

The preliminary WIM calculations, which are done on-site, are discussed in Chapter 4. These calculations include vehicle speed, axle spacing, and wheel weight. Calibration of the weight, pavement roughness, lateral position, and temperature features are described. Data downloading procedures and the Excel macro used to sort, calculate, and summarize data are described.

Different methods of classifying vehicles are described in Chapter 5. Vehicle volume and speed data are discussed, including the variation between lanes, sites, and vehicle classes. Volume and speed trends by day of the week and month of the year are described.

The formulas for calculating ESALs are described in Chapter 6. Some limitations of the AASHO Road Test (e.g., tridem axles and steering axles) are discussed. Axle weight and ESAL statistics and trends are described. A method to estimate and forecast ESALs from vehicle volume and classification data is outlined.

Chapter 7 discusses the data collected with the infrared sensors. The variation of lateral position between vehicle classes and between lanes is described. Lateral position data before and after moving the lane stripes at the north site is discussed. The dual tire data are also discussed.

Installation and calibration of the thermocouples are described in Chapter 8. Daily and seasonal trends are discussed for both the pavement and air temperature.

The final chapter, a summary overview of Chapters 2 through 8, suggests how traffic loading data can be used to plan and design highway pavements.

Chapter 2 Background

This chapter discusses some of the research that has been undertaken to determine causes of pavement damage. In particular, the findings of the AASHO Road Test are reviewed. Other factors that cause or contribute to pavement damage are also discussed. The methods and hardware used in the Highway 59 Research Project to collect traffic data — weigh-in-motion (WIM), inductance loop detectors, and infrared sensors — are discussed as well.

2.1 Causes of Pavement Damage

Traffic loading by heavy vehicles is a leading cause of pavement damage. In this section, the AASHO Road Test, which demonstrated the effects of heavy axle loads, is discussed along with some earlier test roads. Factors other than axle loads, which contribute to pavement damage, are also discussed.

2.1.1 AASHO Road Test

The Bates Experimental Road was a test conducted near Springfield, Illinois, in 1922 and 1923. The test vehicles were trucks with solid rubber tires and wheel loads from 1.1 to 5.9 Mg (2,500 to 13,000 pounds). The results supported the belief in the need to relate pavement design to axle load. The frequency of heavy axle loads increased greatly during and after World War II. Following World War II the American Association of State Highway Officials (AASHO) recommended that states adopt load limits of 8.2 Mg (18,000 pounds) per single axle and 14.5 Mg (32,000 pounds) per tandem axle. By 1950 it was evident that pavements that had served adequately for many years under a limited number of heavy axle loads were being damaged in relatively short periods of time. Road Test One-MD was conducted on rigid pavements in Maryland in 1950 and 1951. The WASHO (Western Association of State Highway Officials) Road Test was conducted on flexible pavements in southern Idaho from 1952 to 1954. Planning for the AASHO Road Test began in 1951, and construction began in 1956 (HRB Special Report 61A 1961; HRB Special Report 61E 1962).

The AASHO Road Test, which was conducted near Ottawa, Illinois, along the future alignment of Interstate 80 from November 1958 to November 1960, showed that the effects

of traffic loading on pavement performance are nonlinear. This is known as the fourth power damage relationship, which means that doubling the axle load results in multiplying the pavement damage by a factor of 16. However, only uniform axle loads were used. Axle loads ranged from 0.9 to 5.4 Mg (2 to 12 kip) for steering axles. Loads on other single axles ranged from 0.9 to 13.6 Mg (2 to 30 kip). Loads on tandem axles ranged from 10.9 to 21.8 Mg (24 to 48 kip). Tire inflation pressures did not exceed 550 kPa (80 psi). There were five loops under traffic, with two lanes per loop and only one axle load combination per lane. The vehicle speeds were set at 48 km/h (30 mi/h) and reduced to 40 km/h (25 mi/h) on the turnarounds. The thickness index or structural number (SN) for the 284 flexible pavement test sections ranged from less than 1 to about 5.7. The surface thickness ranged from 25 to 152 mm (1 to 6 in.), the base thickness from 0 to 229 mm (0 to 9 in.), and the subbase thickness from 0 to 406 mm (0 to 16 in.). The slab thickness for the 268 rigid pavement test sections ranged from 64 mm to 318 mm (2.5 in. to 12.5 in.). To measure the effects of mixed traffic, the equivalent single axle load, or ESAL, concept was introduced so that the damage caused by mixed traffic loads could be described in terms of a standard load. The standard single axle load selected by AASHO was 8.2 Mg (18 kip). Tables and formulas are used to convert axle loads so that the damage caused by a given load is equivalent to that of the 8.2 Mg (18 kip) single axle load. These formulas are discussed in Chapter 6.

2.1.2 Other Factors

Other traffic loading factors that cause or contribute to pavement damage in addition to axle loads are axle-group suspension systems, tire pressure, and tire configuration. Improved suspension systems improve ride quality, which then leads to the use of higher tire pressures. Higher tire pressures result in higher stresses on the pavement surface as the tire contact area is decreased. Most heavy trucks currently have tire pressures 50 percent higher than those associated with the AASHO Road Test. Many heavy trucks have tridem axles in addition to tandem axles. Another factor currently affecting trucks in Texas is the pending implementation of the North American Free Trade Agreement (NAFTA), which permits Mexican trucks to travel on Texas highways. Legal loads in Mexico are higher than those in Texas, and while Mexican trucks are required to observe Texas laws, enforcement of the law is still an issue. Additional factors that accelerate traffic loading damage are roughness, pavement age, poor drainage, and temperature. Roughness leads to greater dynamic loads, as vehicles tend to bounce up and down more. Poor drainage can result in potholes and

cracking, which can then lead to roughness. A large range between extreme high and low temperatures can lead to pavement cracking and roughness. After pavement reaches a certain age, the same load causes more damage than it would have at an earlier age.

Traffic loads are the primary cause of pavement damage, and heavy loads cause much more damage than light loads, as shown by the AASHO Road Test. Other contributing factors include the condition of vehicles and pavement. The next section describes some methods used to collect traffic data.

2.2 Traffic Data Collection

Traffic data, including volume, speed, and weight, are collected for purposes relating to planning, pavement design, and law enforcement. Many different sensing techniques have been used to collect traffic data, with such techniques including pneumatic road tubes, radar, microwave, ultrasonic, video imaging, and piezoelectric cables. The three types of sensors used on the Highway 59 Research Project are WIM, inductance loop detectors, and infrared.

2.2.1 Weigh-in-Motion

Truck weight data have been collected for more than 60 years by means of static scales. Static scales range in size from single-draft vehicle scales used to weigh complete trucks to axle-load scales to wheel-load weighers. Static weighing is inefficient and even dangerous for large numbers of trucks. Another drawback from the standpoint of pavement design is that static scales measure only the gravitational force, not the actual dynamic force exerted on the pavement by the tires of a vehicle traveling at highway speeds.

One of the first efforts to develop a WIM system was undertaken in 1951 by Normann and Hopkins of the Bureau of Public Roads. The first system constructed in Virginia consisted of a 3.0 m by 0.9 m by 0.3 m (10 ft by 3 ft by 1 ft) floating reinforced concrete slab supported by four strain-gauge load cells used for aircraft weighing. Oscilloscope traces were photographed, a process taking 10 seconds for each vehicle. Similar systems were installed throughout the United States, Europe, and Japan through the early 1960s. An inherent problem with the platform WIM systems was that the inertia of the reinforced concrete slab prevented response to rapid changes as required for multiple axles

and closely following vehicles. Other problems included lateral movement, moisture damage, and the expense of construction and maintenance (Cunagin 1986).

Smaller, more portable WIM systems began to be developed soon after the large platform-type scales. Lee developed a system composed of steel plates supported by strain-gauge load cells first at Mississippi State University and later at The University of Texas at Austin. This system, marketed by Radian Corporation, has dimensions of 1,370 mm by 460 mm by 89 mm (54 in. by 18 in. by 3.5 in.). In Germany, a bending plate system was developed that had strain gauges embedded in grooves in the bottom surface of a steel plate. Other WIM systems have included piezoelectric devices, capacitive mats, and strain gauges attached to bridge girders. In the mid-1960s electronic instrumentation became available that greatly facilitated the processing of signals from transducers.

The WIM equipment used in the Highway 59 Research Project was manufactured by PAT (Pietzsch Automatisierungstechnik, GmbH) in Ettlingen, Germany, with United States offices in Chambersburg, Pennsylvania, under the name of PAT Traffic Control Corporation (DAW100 Specifications). These weighpads were selected because they required less excavation of pavement materials and because of their long-term durability and resistance to moisture. The bending-plate weighpads have dimensions of 1,750 mm by 508 mm by 23 mm (68.9 in. by 20.0 in. by 0.91 in.) and weigh 114 kg (251 lb). The steel plates have strain gauges bonded to narrow transverse grooves on the lower surface and are coated with vulcanized rubber, which makes the plates very moisture resistant. Each plate is supported on two edges by a steel frame secured by steel anchors and epoxy within a shallow pit cut into the pavement surface. Lead-in cables from each weighpad are connected to a data processing unit located in an instrument cabinet on the roadside. One weighpad is installed in each wheel path of each lane. When a load is on the weighpad, strain gauges on different parts of the bending plate experience different amounts of strain. The roadside processing unit measures the voltages and calculates the estimated static tire loads, using a proprietary algorithm.

2.2.2 Inductance Loop Detectors

Inductance loop detectors are often used in conjunction with traffic signals to sense the passage or presence of vehicles. An inductance loop detector consists of a loop of wire embedded in the pavement, a lead-in cable, and an electronic detector unit. Inductance is the property of an electric circuit or of two neighboring circuits whereby an electromotive force or voltage is generated or induced in one circuit by a change of current in it or in the other circuit. The inductance of a coil of wire or loop is proportional to the loop area and to the square of the number of turns. Each loop circuit also has an associated resonant frequency that is inversely proportional to the square root of the inductance. If an electrically conductive object, such as a vehicle undercarriage or bicycle frame, enters the magnetic field of a loop, eddy currents are induced in the conductive object. These eddy currents generate a magnetic field opposing the magnetic field of the loop, thus causing a decrease in the inductance of the loop and an increase in the resonant frequency of the loop circuit. The digital detector unit can precisely measure the change in frequency or period and send a signal to a controller unit whenever the threshold is crossed (Kell and Fullerton 1991).

High-bed trucks are more difficult to detect than other vehicles because the eddy currents induced in the undercarriage are more distant from the magnetic field of the loop, and thus cause less of a frequency shift in the loop circuit. A solution would be to increase the sensitivity of the detector unit or to increase the inductance of the loop. Because the inductance is proportional to the square of the number of turns, for the Highway 59 Research Project, a six-turn loop was used instead of the more common two-, three-, or four-turn loop. The size of the loop was 1.8 m by 1.8 m (6 ft by 6 ft).

2.2.3 Infrared Sensors

Infrared sensors have been used for a number of years to collect such traffic data as volume, speed, vehicle length, vehicle height, and headway. An infrared sensor unit consists of a source, a detector, and a control unit. The source, or transmitter, is a light-emitting diode and the detector, or receiver, is a photo-diode. A control unit modulates and demodulates the light sent and received by the source and detector, thus ensuring that operation is not affected by sunlight or other light sources. Infrared sensors can be used in the retroreflective or direct modes, as shown in Figure 2.1. In the retroreflective mode, both the source and detector are

housed in the same unit and the light beam is bounced off a reflector, usually made up of glass beads or corner cubes. In the direct mode, the beam is not reflected, and the source and detector are housed in separate units. The advantage of the direct mode is that the detector receives a much more powerful light beam because no light is lost with a reflector, and the distance traveled by the light beam is not doubled. The disadvantage of direct mode sensing is that extra cables must be used, sometimes in a difficult location. When infrared sensors are used to measure traffic, they can sense the beam blockage by either the vehicle bodies or the vehicle tires. If tires are being measured, then the light beam must travel very close to the surface of the road, and one of the sensors or a retroreflector sheltered within a very rugged housing must be placed on the pavement surface in the center of the lane. If the source or detector is on the pavement surface, the cable running back to the edge of the road must be protected from contact with vehicle tires.

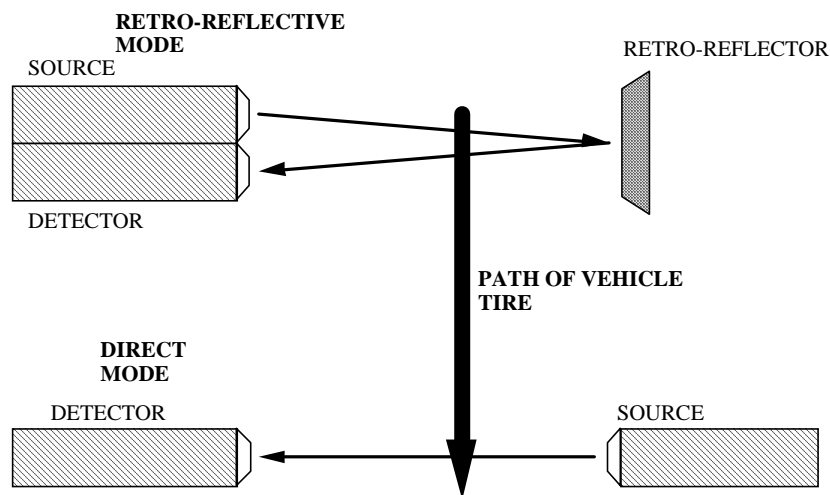


Figure 2.1 Infrared Sensing Modes

On previous research projects near Jarrell, Texas, and with the Oklahoma Turnpike Authority outside Oklahoma City, infrared sensors were used to measure the passage of vehicle tires. In both projects retroreflectors were placed on lane-marker-type buttons that were attached to the pavement surface in the center of the lane. While the systems worked satisfactorily over the short term, road film built up on the retroreflectors, which required frequent cleaning.

Direct-beam infrared sensors were selected for the Highway 59 Research Project because they function well even when the lenses are very dirty, and it was possible to route the cables for the sources underneath the weighpad frames. The sources and detectors used for this project are externally identical with an outside diameter of 7.92 mm (0.312 in.). The effective light beam is 14 mm (0.55 in.) and the maximum range is 112 m (369 ft). The wavelength of the infrared light beam is 880 nm. The sensors were manufactured by Opcon, Inc., with headquarters in Everett, Washington (Opcon Industrial Sensors Catalog 1990; Garner, Lee, and Huang 199; Garner and Lee 1995).

In this chapter, some of the background related to causes of pavement damage has been discussed. The AASHO Road Test showed that axle loads are the primary cause of pavement damage. The hardware systems used for the Highway 59 Research Project to collect traffic loading data are WIM, inductance loop detectors, and infrared sensors. The installation and maintenance of these traffic-data sensors at the research project site in east Texas are discussed in the next chapter.

Chapter 3 Equipment Installation and Maintenance

The project background and construction of the Highway 59 pavement test sections in east Texas are discussed in this chapter. The installation and maintenance of the weigh-in-motion (WIM) system is also described.

3.1 Highway 59 Rehabilitation Plan

The Highway 59 Research Project includes the design, construction, and monitoring of two pavement test sections on Highway 59 near Corrigan, Texas. One test section comprises seven segments of flexible pavements, and the other, seven segments of rigid pavements. A WIM system was installed in the control segment of each test section.

3.1.1 Test Sections

US Highway 59 in Texas is located in an important transportation corridor that connects the U.S. midwest and east Texas with Houston, south Texas, and Mexico. Historically the pavements on Highway 59 in the Lufkin District of the Texas Department of Transportation (TxDOT) have required much maintenance and reconstruction. In an attempt to find ways of reducing the total life-cycle cost of pavement in the district, a research study was commissioned for the development of a long-range rehabilitation plan. The research project included designing, building, and monitoring two pavement test sections in the southbound lanes of Highway 59 about 50 km (30 mi) south of Lufkin and 160 km (100 mi) north of Houston. One test section (rigid pavement) is located 6 km (4 mi) north of Corrigan, and the other test section (flexible pavement) is located about 3 km (2 mi) south of Corrigan. US Highway 287 intersects Highway 59 in Corrigan, where TxDOT has a maintenance facility. The north, or rigid, pavement test section comprises a jointed concrete pavement that was constructed in 1936 and has been overlaid several times with asphalt overlays that now total about 180 mm (7 in.). The south, or flexible, pavement test section was built in 1966 and has been overlaid several times, also with a total asphalt thickness of 180 mm (7 in.). In the north section, reflective cracking was the most common sign of distress, while at the south section, longitudinal and transverse cracking were common indicators (Cho and McCullough 1995).

Each test section is 2.1 km (7,000 ft) long and comprises seven 300 m (1,000 ft) segments, each of which was reconstructed with a different treatment (structural make-up). The southernmost 300 m (1,000 ft) segment of each test section is a control section that received no reconstruction treatment, as it is considered to be representative of the respective, existing pavement structures. However, in the final stage of reconstruction, all segments, including the control segments, received an asphalt overlay.

The rigid pavement test segments at the north site are named R0 through R6, with R0 being the control segment. Segments R1 through R3 had the existing asphalt overlays milled off. Before new overlays were placed, the remaining pavement in Segment R1 had the cracks and joints repaired and sealed, while a large hammer was applied to the remaining pavement in Segment R2 to break up the concrete slabs and seat the pieces onto the subgrade. A flexible base material was applied over the milled surface in Segment R3. An open-graded asphalt mix followed by a binder course was placed over the unmilled pavement of Segment R4. A stress-relief interlayer was placed on the existing surface of Segment R5 before a new overlay was placed. Thus, Segments R1 through R5 received new asphalt overlays of various thicknesses, along with other treatments, while Segments R6 and R0 received only a final asphalt overlay.

The 300-m (1,000-ft) long segments at the flexible pavement test section south of Corrigan are named F0 through F6, with F0 being the control segment. Segments F1 through F4 received similar thickness treatments with different combinations of aggregate and asphalt binders over the existing flexible pavement. The old overlay material was milled off Segments F5 and F6 and replaced. Flexible base material followed by an asphalt overlay was applied on Segment F5 while Segment F6 received two different types of asphalt overlay treatment. Segment F0, the control segment, received only a final asphalt concrete overlay.

After reconstruction, every 300-m (1,000-ft) long pavement segment has a different structural number (SN) associated with it. The SN, which is used in calculation of equivalent single axle loads (ESALs) is, for flexible pavements, a function of the stiffness and thickness of each layer and describes the effective overall strength of the composite layers (AASHTO Guide for Design of Pavement Structures 1993). Depth of the concrete pavement slab is normally used instead of the SN in ESAL calculations for rigid pavements, but because the rigid pavement test segments already had asphalt overlays, it was necessary to use composite

SNs to characterize the strength of the overlaid concrete pavements. The composite SNs used to describe the overlaid rigid pavement test segments ranged from 4 to 11 and, for the flexible pavement test segments, from 6 to 8. For SNs greater than about 7, the results from ESAL calculations are relatively less sensitive to the value of SN than for values less than this.

3.1.2 Traffic and Temperature Monitoring

A WIM system was installed in the control segments (F0 and R0) at both test sections to measure traffic loads. Traffic data from the WIM systems for vehicles in each southbound lane include number of vehicles, wheel loads, speed, number of axles, axle spacing, lateral position, and indication of single or dual tires. The WIM instrument systems were also used to measure and record the air and pavement temperatures every hour.

The systems have operated continually since their installation in 1992 and have monitored the passage of every southbound vehicle, including passenger cars, except for an occasional equipment or communication malfunction. A data file is generated, with respect to time, for each vehicle and stored temporarily on-site by the WIM instrument at the roadside. Periodically, these data files are transferred via modem over a local telephone line to a microcomputer at the Corrigan maintenance facility. Accumulated files are then transferred from the microcomputer to disks, and the disks are mailed to the Center for Transportation Research at The University of Texas at Austin for data processing.

This is probably a unique data set, not only in its continuity and range of measured and calculated pavement-loading parameters (loads induced by traffic and by temperature change), but also in its direct association with the effects that the observed traffic loads and temperature changes have upon the performance of the adjacent pavement test sections. Traffic, temperature, and pavement performance have all been monitored at the two test sites over an extended period of time.

3.1.3 Pavement Monitoring

Pavement performance evaluation includes both serviceability, or ride quality, and structural capacity. Present serviceability, i.e., the ability of a specific section of pavement to

serve high-speed, high-volume mixed traffic in its existing condition, is commonly described quantitatively by a present serviceability index (PSI) (Huang 1993). The objective measurements that comprise this index include longitudinal profile, rut depth, and cracking and patching. Longitudinal profile has been found to be a major contributor. Longitudinal surface profile, a direct indicator of ride quality, can be measured with an inertial profilometer, which incorporates an accelerometer on the vehicle body plus a pavement surface probe (wheel on a spring-loaded trailing arm or a noncontact device) in each wheel path. The profilometer vehicle can travel at speeds up to about 70 km/h (45 mi/h). The relative distance between the pavement surface and instrumented vehicle body is measured with respect to time and speed (horizontal distance). This value is added to the second integral of the vertical acceleration of the vehicle body to give the pavement surface profile relative to an imaginary horizontal plane.

Structural capacity can be estimated from the results of tests on core samples taken from the pavement or from the interpretation of deflection measurements made after a load is applied on the pavement surface (nondestructive testing). Such deflection measurements can be obtained by a falling weight deflectometer, an instrument that drops a weight onto a pavement surface contact pad and records the relative vertical movement of selected points near the area of impact. Rut depth is measured vertically from a transverse straightedge with a ruler. Cracking and patching are manifestations of pavement distress and are used to imply changes in structural capacity. Pavement cracking is surveyed visually, and records are made of the number, length, width, and type of cracks that show on the pavement surface at the time of observation. Common crack types are reflection cracks, which may run transversely or longitudinally, and fatigue or alligator cracks. Pavement condition surveys also include such other distress manifestations as patching, pumping of water through cracks, material segregation, spalling, joint-faulting, and raveling.

Pavement performance should be monitored periodically throughout the lifetime of a pavement. In the case of this research project, pavement performance surveys were made before, during, and at regular intervals after reconstruction of the test sections.

The background of the Highway 59 pavement test sections was described in this section. A WIM system collects traffic load and temperature data continuously at both

sections. Pavement performance data, including roughness, rut-depth, and cracking, are collected periodically.

3.2 Test Section Construction and WIM Installation

This section gives a brief history of the construction of the Highway 59 test sections. The installation of the WIM systems is described in some detail.

Detour construction at the rigid pavement test location north of Corrigan began early in the fall of 1991. The dates for the major construction and maintenance events are listed in Table 3.1. Both southbound lanes were closed, and the traffic was diverted across the median to the two northbound lanes where a median barrier had been installed between the two lanes to form one northbound and one southbound traffic lane through the 2.1-km (7,000-ft) detour. In September 1991, while the test pavements were being built, drainage conduits for the WIM tire-force sensors (weighpads) were placed into the existing pavement near the middle of Segment R0. The positions of junction boxes at strategic points in the conduit were surveyed for subsequent relocation after a 38-mm (1.5-in.) overlay had been placed in the final stage of test pavement construction, and before installation of the WIM weighpads. The galvanized steel drainpipes also serve as conduits to carry the weighpad and infrared sensor cables to pull-boxes just off each shoulder.

In March 1992, soon after the overlay was placed, the weighpads were installed by a crew from TxDOT in Austin. Saw-cuts were made at the surveyed locations, and pneumatic tools were used to remove the asphalt concrete between the saw-cuts to a depth of about 50 mm (2 in.). Additional holes were drilled into the pavement for anchor bars. Steel base plates to accommodate the infrared sensor sources were field-welded to one corner (center of lane) of two weighpad frames. The weighpad frames were then positioned and leveled with special alignment devices. Epoxy was placed around and under the frame and in the anchor holes. The weighpads were set in the frames with shims underneath the transverse edges such that the tops of the weighpads were flush with the pavement surface. The lead-in cables for both the weighpad and infrared sensor sources were routed under the weighpad frame and to the roadside pull-boxes through the steel drainage conduits.

The infrared source was secured inside a custom-made metal raised-pavement-marker button that was bolted to the steel base-plate that had previously been welded to the weighpad frame. Figure 3.1 shows the housing used for the infrared source. A more detailed view of the infrared source/receiver unit is shown in Figure 3.2. Figure 3.3 shows the weighpad frame with base plate. The infrared sensor receiver was housed inside a pipe nipple that was attached to a short post driven into the ground just off the shoulder. Inductance loop detectors were also placed in the center of each lane in advance of the leading weighpads. The loops were 1.8 m by 1.8 m (6 ft by 6 ft) with six turns of stranded, insulated wire in a protective sheath. The larger-than-usual number of turns was used in an attempt to detect high-bed trucks, especially logging trucks, which are prevalent in the area. A test loop had been installed north of Livingston near a rest area in January 1992 where a series of tests was run to determine the most appropriate loop size and number of turns.

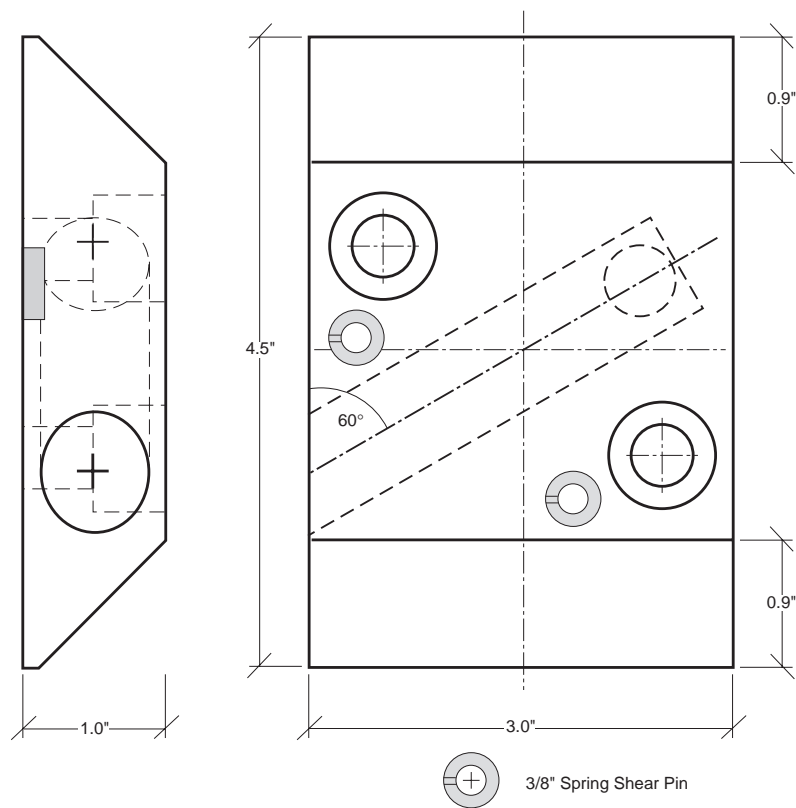


Figure 3.1 Housing for Infrared Source

1 in. = 25.4 mm

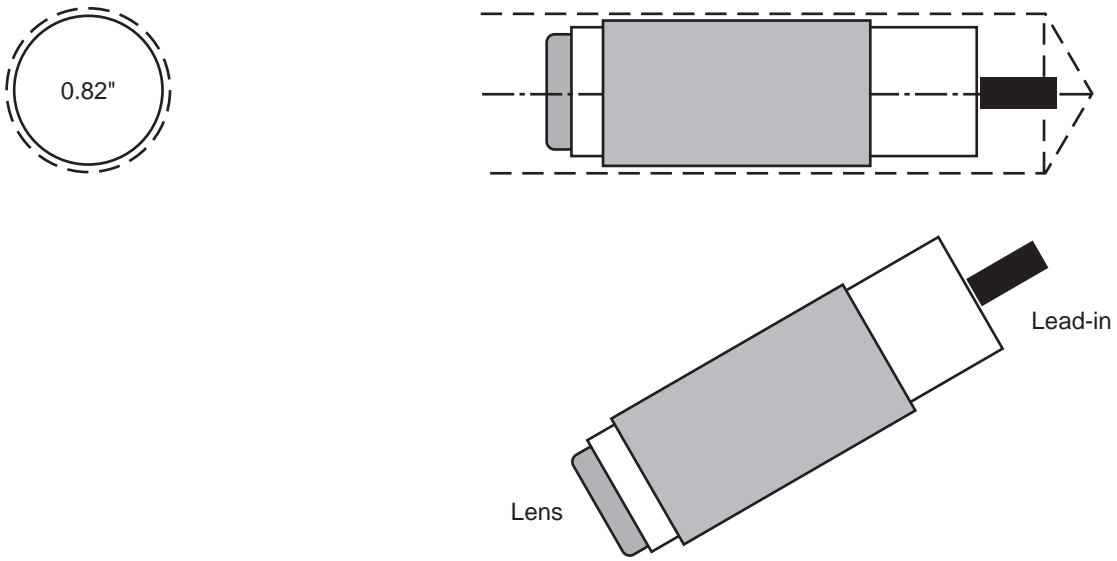


Figure 3.2 Infrared Source/Receiver Unit

1 in. = 25.4 mm

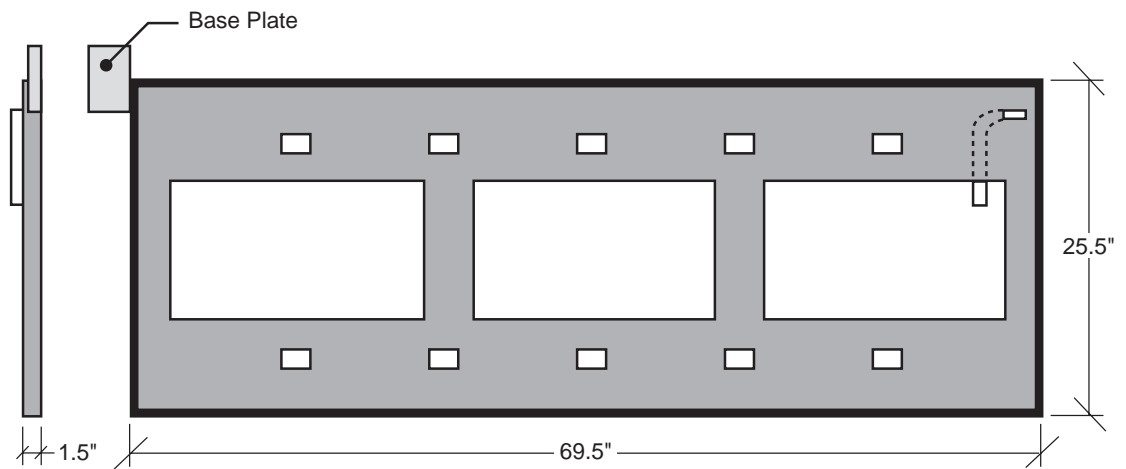


Figure 3.3 Weighpad Frame with Base Plate for Infrared Source

1 in. = 25.4 mm

The north pavement test site was opened to traffic in April 1992; however, it was soon discovered that the longitudinal paint stripes marking the lane edges had been placed by the Lufkin District paint striping crew in the wrong lateral location. The position error ranged from about 200 mm to 500 mm (8 in. to 9 in.). These stripes were either removed or painted over in black and then repainted in the correct positions a year later in April 1993.

At the flexible pavement test site south of Corrigan, the across-median detour pavements failed after only a few hours of traffic, and it was necessary to construct the test pavements one lane at a time. Instead of diverting the traffic across the median, as had been done previously at the rigid pavement test site north of Corrigan, traffic sign, cones, and barrels were used to guide traffic into one of the southbound lanes adjacent to the construction work zone.

Drains for the WIM sensors were installed at the south site in June 1992. The entire flexible pavement test section was overlaid immediately thereafter, the weighpads were installed, and the section was opened to traffic in July 1992. In August 1992 the first software chip or erasable programmable read-only memory (EPROM) had been installed in the WIM instrument system at the north site. The first EPROM was installed at the south site in October 1992. However, it was necessary for the WIM-system vendor to make modifications to the supplied software after some inadequacies were discovered, and the second set of EPROMs was installed in November 1992. At this time the systems at both sites were calibrated using a three-axle test truck with known axle loads, which made repeated runs over the sensors at several different speeds.

Continuous data collection began at both pavement test sections in December 1992. An IBM-compatible 286 computer with internal 2,400 baud modem was set up in TxDOT's Corrigan maintenance facility office and was programmed to automatically download data by the local telephone line to the computer's hard disk at selected times in the evening. About every two weeks, an engineer from the Lufkin District would copy the accumulated binary-code data files from the hard disk to floppy disks and mail the disks to Austin. This procedure was deemed necessary, as the long-distance telephone charges for downloading the 8,000 or so daily vehicle records for each site directly to Austin (approximately 20 minutes per day) seemed excessive. In April 1993, EPROMs containing the third software version

were installed, and temperature data collection began at both sites, along with the WIM data mentioned previously.

Table 3.1 Construction and Maintenance History

8 August 1991	Site selection
13 September 1991	North: drain installation
7 January 1992	Test loop near Livingston
4–10 March 1992	North: weighpad installation
19 April 1992	North: open to traffic
26 May 1992	South: drain installation
7,8 July 1992	South: weighpad installation
31 August 1992	North: site begins operation
9 October 1992	South: site begins operation
9–10 November 1992	Calibration with three-axle truck
19 November 1992	EPROM for storing IR data
1 December 1992	Begin continuous data collection
25 January 1993	South: temperature calibration

Table 3.1 Construction and Maintenance History (continued)

8 February 1993	North: temperature calibration
2 April 1993	North: new EPROM to improve transmission speed
15–22 April 1993	North: stripes removed and replaced
19 April 1993	South: new EPROM for improved transmission
	North: premix pavement repair
19 May 1993	South: right-lane IR source replaced
8–10 August 1993	Calibration with five-axle truck
	Lateral position calibration and straightedge
24–25 August 1993	New EPROMs to suppress rolling records
	North: modem power supply bad
	South: left-lane IR source water damage
9–10 September 1993	North: modem not working
	South: left-lane IR source replaced
14–15 October 1993	More modem problems
	South: main power supply removed
5 November 1993	South: main power supply restored
13 December 1993	US Robotics modems set up
7 June 1994	North: new IR sources both lanes
1 July 1994	North: right-shoulder IR detector reinstalled
14 September 1994	North: riser plate beneath right-lane IR source installed
29 September 1994	South: left lane source gone
October 1994	Flooding; north site under water
3–4 November 1994	South: left-lane IR source replaced

This section has described the construction of the test sections and the installation of the WIM systems. The major events with respect to traffic data collection on the Highway 59 Research Project are listed in Table 3.1.

3.3 Maintenance and Repair

This section describes the maintenance and repair of the infrared sensors and modems used on the Highway 59 Research Project. The weighpads have not required any maintenance other than calibration. At the north site the pavement began to spall around the corners of the inductance loops and there was some shoving in the left wheel path of the left lane. Premix asphalt was used to patch the shoving and an asphalt-sand mixture was used to fill in the gaps around the loop wires in April 1993. In the same month, the lane stripes at the north test section were painted over and repainted in the correct location. After a flood in October 1994, the north site inductance loop detectors began working erratically, while other problems developed with the DAW100 main board. These problems were finally resolved in March 1995.

3.3.1 Infrared Sensors

The original lane-marker-button type infrared source housings were attached to a base-plate welded to the weighpad frame with two 9.5-mm (0.375-in.) bolts and sealed around the edges with caulk. Terminal strips connected the lead-in cables. Later, these housings were modified to include two 9.5-mm (0.375-in.) shear pins, and the lead-in wires were connected with epoxy splicing kits. The infrared source in the right lane at the south site was replaced in May 1993 after the bolts sheared off. The new lane marker button included shear pins. The infrared source was replaced in the left lane at the south site in August 1993. The problem here seemed to result from water seeping up through the drain, rusting the terminal strip, and shorting out the electrical connections. In June 1994 both of the sources at the north site were replaced with new sources incorporating shear pins. The connections were spliced and sealed with epoxy and caulk. The original infrared sources lasted 10 months and 13 months in the right and left lanes, respectively, at the south site, and 26 months at the north site. In September 1994, the left lane source at the south site was knocked loose; it was replaced in November 1994. Serious flooding occurred in October 1994. The highway north and south of the north site was under water and possibly the site itself was submerged. At one point a car ran off the road and damaged the post holding the infrared receiver on the shoulder. At least twice, a mower damaged the posts. During the summer months, especially, grass grew up in front of the receivers and needed to be uprooted

or sprayed with herbicide. Also, at one location, spiders built webs inside the tube and blocked the beam. The infrared sensors performed well during light rain. They were not observed during heavy rain; snow and ice did not occur during the observation period.

3.3.2 Modems and Software

The first software version, installed in August 1992, displayed real-time infrared sensor data but did not store infrared data. The second software version, installed in November 1992, included the storage of infrared data. The first set of modems used was manufactured by Practical Peripherals and was rated at 9,600 baud; however, the effective transmission rate was much lower because much unnecessary data were stored in an inefficient format. Because of the slow transmission speed, the length of the data files, and the cost of long-distance telephone service to Austin, an IBM-compatible 286 computer was set up in the TxDOT maintenance facility office in Corrigan and programmed to automatically download data from each site after working hours. Every two to three weeks an engineer from Livingston, usually Eric Starnater, copied the data files to floppy disks and restarted the automatic download program. In April 1993, new EPROMs were installed that stored only the essential data in a more efficient format, which resulted in a significant increase in transmission speed. During the summer months of 1993, many *rolling records* were produced each day. A rolling record or *phantom vehicle* is the term used for records having default weights and axle spacings which were often generated between genuine vehicle records, perhaps as a result of the loop detector giving false signals. These records could easily be sorted out; however, they greatly increased the size of the raw data files and the data transmission time. In August 1993, new EPROMs were installed to suppress the storage of vehicle records with default dimensions. Also during the summer of 1993, the Practical Peripherals modems began to work erratically, possibly because of heat or voltage surges occurring during thunderstorms. Both electricity and telephone lines had surge suppressors installed, and small fans were installed in the cabinets to circulate air. Sometimes after switching off, then on again, the modems worked for a few weeks. Twice the modems were returned to the manufacturer to be replaced. After numerous trips from Austin to Corrigan to try to solve the modem problem, it was decided that this model was not suited for roadside use. More rugged modems made by US Robotics were purchased and installed in December 1993. These have continued to run through 1994 without any serious problems.

The construction of the Highway 59 pavement test sections and the installation and maintenance of the WIM systems used to collect traffic data have been described in this chapter. The major construction and maintenance events are listed in Table 3.1. After installation and calibration of the equipment, most of the trips to Corrigan in 1993 involved software problems and modem failures. Most of the trips in 1994 involved replacing or realigning infrared sensors. The weighpads have not required any maintenance other than calibration.

Chapter 4 Data Acquisition and Analysis

The preliminary data analysis that is done on-site at the Highway 59 Research Project is discussed in this chapter. The on-site data processing includes speed, axle spacing, and weight. The calibrations for weight, pavement roughness, lateral position, and temperature are described. The Excel macro used to sort, analyze, and summarize the data is discussed.

4.1 Preliminary Calculations

A PAT model DAW100 instrument unit in a roadside cabinet processes the signals from four weighpads, two inductance loop detectors, two infrared sensors, and two thermocouples. The PAT software calculates weight, speed, and axle spacing for each vehicle from the weighpad output signals on-site. Lateral-position and dual-tire data are calculated later from the infrared sensor signals that are stored and displayed as milliseconds. Temperatures are also calculated later from the thermocouple signals that are stored and displayed as ohms of electrical resistance.

4.1.1 Speed and Spacing

Staggered weighpads were used at the Corrigan, Texas, site to measure the speed and axle spacing more accurately. In the past, two inductance loops have been used in each lane to calculate speed and overall length of vehicles. However loops tend to lose logging trucks and other vehicles without large masses of metal near the pavement surface. The weighpads in each lane are staggered longitudinally 4.6 m (15 ft) to establish a reference distance for speed calculations. The layout of the weighpads, loops, and infrared sensors is shown in Figure 4.1. The speed of each axle is calculated as the distance between weighpads divided by the time for that axle to cross each weighpad. Normally, vehicle speed is assumed to be constant, and only the speed of the first axle of each vehicle is calculated. The spacing between axles is then calculated by multiplying the speed with the time interval between each axle crossing one weighpad. The inductance loop is not used for speed calculations; it simply alerts the leading weighpad that a vehicle is about to cross.

An inductance loop in advance of the leading weighpad signals the computer to begin recording time and weight signals from the weighpads. A time delay is added in order for the

entire vehicle to cross both weighpads. The loop measures 1.8 m by 1.8 m (6 ft by 6 ft) and has six turns so it will be more sensitive to logging trucks, which are very common in the area. The speed for each axle can be measured independently. To calculate the axle spacing, the average speed of the two axles can be used if the vehicle is accelerating.

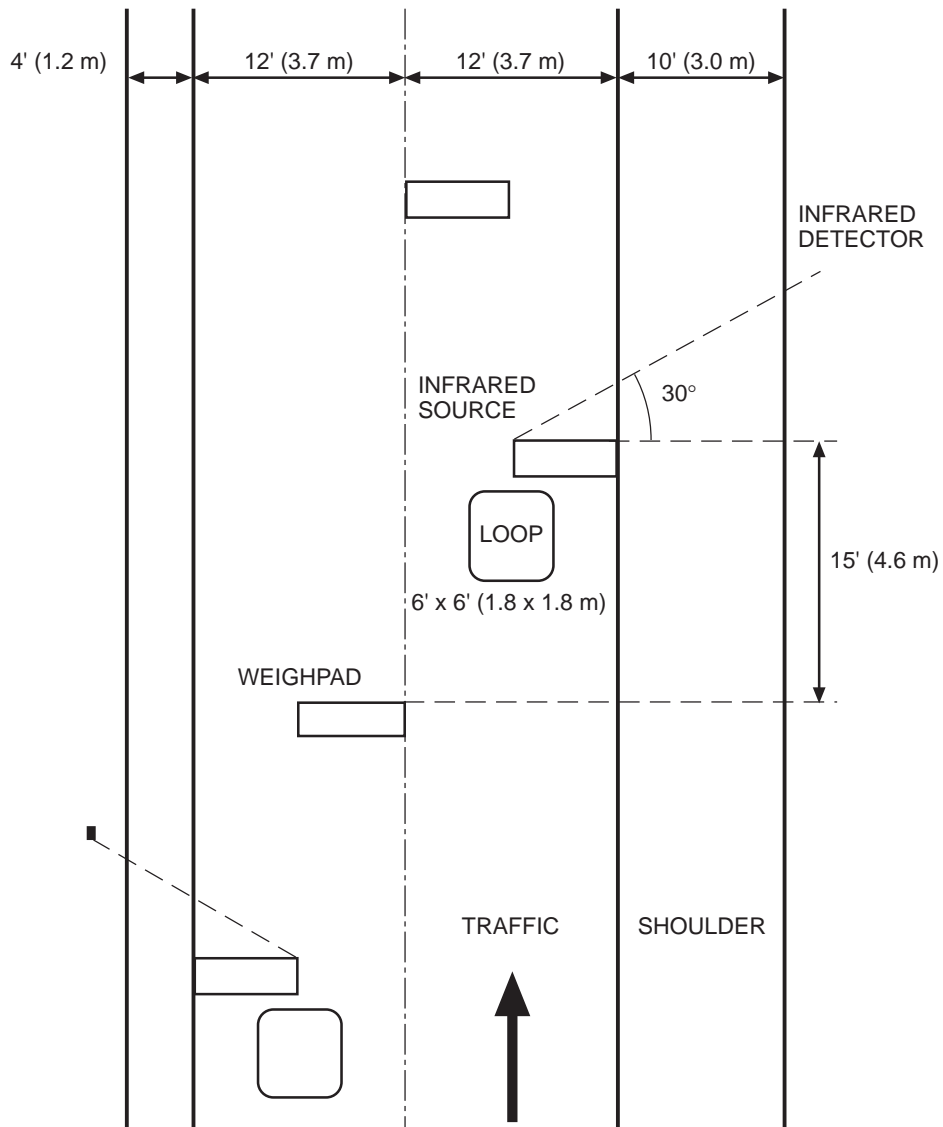


Figure 4.1 WIM System Layout

4.1.2 Lateral Position and Dual Tires

The infrared source, or transmitter, is attached to the corner of the leading weighpad in each lane, as shown in Figure 4.1. The infrared receiver, or detector, is located off the shoulder in such a way that the infrared light beam forms a 30° angle with respect to the transverse edge of the weighpad. Lateral position signals are stored in milliseconds as the time from the front tire crossing a point on the weighpad to the time the tire breaks the infrared light beam. This time interval is multiplied by the vehicle's speed, and the ratio of the sides of the triangle formed by the infrared light beam and the edge of the weighpad is used to calculate a lateral distance between the tire and the lane edge. This distance is adjusted to account for the location of the tire on the weighpad when a weight value threshold is exceeded. The lateral position is measured with respect to the edge of the lane; so the right-lane lateral position is the distance of the front tire from the right edge of the lane, and the left-lane lateral position is the distance from the left edge of the lane.

The length of time the infrared light beam is interrupted by each tire can be used to determine whether the tire is single or dual. The first tire of every vehicle is assumed to be single; subsequent tires are indicated as dual if their infrared light beam interrupt times are more than 20 percent greater than that for the first tire. Right-side tires are measured in the right lane and left-side tires are measured in the left lane.

4.1.3 Real-time Display

Each vehicle record can be viewed in real time either on a laptop computer on-site or remotely via modems and a telephone line. An example of a three-axle vehicle record is shown in Table 4.1. The vehicle number denotes how many vehicles have passed since midnight. Lane 2 indicates the left lane and Lane 1 the right lane. The infrared time in the total column is the time used to calculate lateral position. The other infrared times are used for dual-tire indication. On separate screens, additional data can be viewed, such as the calibration settings, the status of files stored in memory, thermocouple readings, and diagnostic information, which can be used during system setup or to aid in troubleshooting problems with the loop detectors or weighpads. On a few occasions after resetting the loop detector, the real-time vehicle data were compared with manual observations to confirm that the axle number and axle-spacing pattern for each vehicle were correct.

Table 4.1 Real-time Vehicle Data for Three-axle Vehicle

1 mi/h = 1.609 km/h

1 kip = 0.4536 Mg

1 ft = 0.3048 m

Veh. No.	Lane	Date	Time	Speed	Gross Weight	
3596	2	25-8-93	13:53:42	66 mi/h	20.0 kip	
Axle No	Total	1		2		3
IR Time	32 ms	14 ms		19 ms		19 ms
Right Load	10.1 kip	3.9 kip		2.8 kip		3.3 kip
Left Load	9.8 kip	3.8 kip		2.7 kip		3.2 kip
Spacing	18.3 ft		13.8 ft		4.5 ft	

The layout of the WIM system and the preliminary data analysis, which was done on-site by the PAT software, are discussed in this section. Speed, axle spacing, wheel loads, and infrared times are some of the data that can be viewed in real time.

4.2 Calibration

Calibration of the weighpads to obtain accurate speed, axle spacing, and weight is discussed here. A straightedge was used to measure pavement roughness before and after the weighpads. Lateral position and temperature measurements were also calibrated.

4.2.1 Weight

The first calibration of the weighpads was performed in November 1992. A three-axle test truck and driver were provided by the Texas Department of Transportation. Each axle-group on the truck was weighed on a vehicle scale at a commercial weigh station and the spacing between axles was measured with a tape. Multiple runs were made by the test truck in each lane at speeds ranging from 56 km/h (35 mi/h) to 105 km/h (65 mi/h). The first few

runs were performed to adjust the indicated speed and axle spacing to agree with measured values of axle spacing on the test truck. Adjustments were made to the PAT software by typing in new values for the effective distance between the staggered weighpads. Preliminary adjustment factors were set for each weighpad and for each lane. Additional factors were set for three different speeds: 72, 88, and 105 km/h (45, 55, and 65 mi/h).

In August 1993, both a five-axle test truck and the original three-axle test truck were used to confirm the calibration factors. The weight calibration was done at speeds of 72, 88, and 105 km/h (45, 55, and 65 mi/h) in each lane. The axle spacings were measured and the wheel loads weighed at a static scale. One weighpad factor was adjusted to weigh the five-axle truck correctly. The factors for other weighpads did not require adjustment.

4.2.2 Pavement Roughness

An accurate WIM system requires a smooth road surface before and after the weighpads to reduce as much as possible the effect of bouncing vehicles. A 6-m (20-ft) straightedge was assembled from three sections of aluminum pipe and tensioned with cable. This straightedge was used to measure pavement roughness for 30 m (100 ft) in advance of and beyond the weighpads at the time of installation and later during the weighpad calibration. A 150-mm (6-in.) diameter, 3.2-mm (0.125-in.) thick feeler plate was used to search for gaps underneath the straightedge. Some rutting in the wheel paths was observed in August 1993.

4.2.3 Lateral Position

The lateral position calibrations were performed by painting the metal edge of the weighpad with flat black paint and then smearing this with oil. An observer measured the position of the tire tracks of passing vehicles on the oil-covered surface. It was difficult to observe the precise position of the first axle of five-axle trucks because the tracks were obscured by the following dual wheels. The three-axle test truck was observed during the weighpad calibration described above because it was possible to stand closer to the weighpad. Passenger cars were also observed. The PAT software displays the lateral position in milliseconds. The lateral positions calculated from the infrared times were correlated with the observed lateral positions.

4.2.4 Temperature

The temperature calibration was performed by immersing the thermocouples with a thermometer in a container of ice water and heating over a gas burner up to 60°C (140°F). The thermocouples are connected to the main board of the PAT system and the readings can be accessed in real time by a computer. The thermocouple readings are saved once an hour and are a part of the raw data file for each day.

Calibration for weight, roughness, lateral position, and temperature have been described. Three-axle and five-axle test trucks were used to calibrate the WIM system, and a straightedge with feeler plates was used to measure pavement roughness. These calibrations should be done on an annual or semiannual basis. It would be useful if the lateral position of the front axle of five-axle trucks could be observed and measured more precisely.

4.3 File Management and Sorting

In this section, the procedures used to transfer the raw data files from the roadside processing unit to the maintenance facility in Corrigan, and then to Austin, are described. An Excel macro was used to classify vehicles, calculate ESALs and lateral position for each vehicle, and summarize all the vehicle records for each day.

4.3.1 Data Downloading

Four megabytes of memory were available on site in the DAW100 unit, which is sufficient for 12 to 17 days, depending on traffic volume. The data could be downloaded directly to a laptop PC on the roadside or remotely by a modem over the telephone line to a PC in Corrigan or in Austin. The maximum baud rate was 9,600 bits per second, which means a week of data could take three hours or longer to transmit over the phone line. To reduce the number of long distance telephone calls, a PC with an internal modem was placed in the Corrigan maintenance facility and was programmed to automatically download data from both sites after working hours. Once or twice a month the data files were copied to floppy disks, usually by Eric Starnater, a TxDOT engineer. The floppy disks were mailed to Austin, and the automatic download program was reset.

4.3.2 Excel Macros

All the temperature and vehicle data at each site for each day were stored in one data file in a binary format. The raw data files had an average size of about 300 kilobytes. A translation program written by Liren Huang was used to translate each binary file into ASCII format that resulted in a temperature file and a very large vehicle file, about 600 kilobytes. The data for each vehicle were in one line so each vehicle file had an average of 7,000 lines. An Excel macro was written to sort, analyze, and summarize the data. The first stage in the sort routine was to sort out all the vehicle records with obvious errors, e.g., axle spacing over 18 m (60 ft) or less than 0.6 m (2 ft), speeds in excess of 160 km/h (100 mi/h), and phantom vehicles. Phantom vehicles had default axle spacing and weight values and seemed to be created by the PAT software whenever the loop detector remained in the on position after a vehicle passed. Phantom or ghost vehicle records were especially problematic at the south site in the summer months and resulted in very large binary data files (600 kilobytes or more). Later, the PAT software was changed so that phantom vehicle records were not stored in the binary data file, although they could still be observed on the computer screen in real time. The second stage in the sort routine was to separate the vehicles into different files depending on the vehicle class. Initially, the number of axles was used as the criterion to classify vehicles. The two-axle file was the largest and the five-axle file was the second largest for each day. The three-, four-, and six-or-more axle files for each day were quite small in comparison. The two-axle file could be further subdivided into a truck and passenger car file depending on the axle spacing; this was done for files after 1993.

The next part of the Excel macro calculated ESALs and lateral position for each vehicle. The ESALs for two-axle vehicles could be calculated in one step because both axles were singles. The ESALs for three-axle vehicles and larger were calculated individually for other than the steering axles as a determination was required about whether the axles were single, tandem, or even tridem. The lateral position calculation was different for each lane so it was calculated separately for each vehicle. The steering axle ESALs, the gross vehicle weight, and the dual tire indication could be calculated in one step for each file. More detailed descriptions of these calculations will be given in Chapters 6 and 7. After all the calculations were completed for each vehicle, each file was sorted by lane number and summarized. A separate summary file for each day was created which contained the

summarized data from the files for each vehicle class. An example of a summary file is shown in Table 4.2. The summary data include volume, average speed, average lateral position, total weight, total ESALs, and total dual tires for each vehicle class for each lane. Beginning in December 1993, the two-axle vehicle class was divided into two classes, one with axle spacing less than 3.4 m (11 ft), and the other with larger axle spacing.

Table 4.2 Summary File for 31 December 1993

1 mi/h = 1.609 km/h

1 kip = 0.4536 Mg

1 ft = 0.3048 m

Site	Year	Month	Day	Pt	SN	
2	1993	12	31	2.5	6	
(south)						
Right Lane						
	Volume	Speed, mi/h	Load, kip	ESALs	Lateral Position, ft	Dual Tires
2-axle, sp < 11	3,489	65	13 243	22	3.50	174
2-axle, sp > 11	1,095	65	6 166	24	3.10	182
3-axle	105	63	1 352	11	2.93	48
4-axle	125	62	1 909	12	2.84	50
5-axle	507	63	25 632	473	2.76	489
6-or-more axles	7	66	438	13	1.78	7
Total	5,328	65	48 740	556	3.31	950
Left Lane						
	Volume	Speed, mi/h	Load, kip	ESALs	Lateral Position, ft	Dual Tires
2-axle, sp < 11	1,626	67	6 440	12	3.65	11
2-axle, sp > 11	548	67	2 617	10	3.56	38
3-axle	26	67	330	3	3.27	11
4-axle	43	65	538	3	3.18	16
5-axle	78	67	3 716	70	2.11	74
6-or-more axles	2	68	31	< 1	2.54	< 1
Total	2,323	67	13 671	98	3.57	150

Originally the data-processing program was a set of four Excel macros with a total length of about 2,000 lines. The time to process one file from start to finish averaged about 30 minutes, using an IBM-compatible 486 computer. Later versions of the program and an

IBM-compatible Pentium computer reduced the average processing time to less than 10 minutes. A few days of very high traffic volumes took much longer to process. All the processed files for one day from one site could almost always be stored in ASCII format on one high-density floppy disk (1.4 Megabytes). The files could also be compressed and stored on other electronic media.

Two months — June at the north site and December at the south site — had no missing days. August and March had the most missing days at the north site, with 24 and 15 missing days, respectively. April and March had the most missing days at the south site with 15 and 13 missing days. The problem in most cases was the modem not working properly; a few times the erasable programmable read-only memory (EPROM) did not work properly. Sometimes the data file was saved but with some parts unreadable, possibly because of transmission difficulties. Total missing days were 93 or 25 percent at the north site, and 88 or 24 percent at the south site. Sundays and Mondays were the most frequently missed days, while Tuesdays and Saturdays were least frequently missed.

Missing volume, weight, ESAL, and dual-tire data were interpolated by averaging the values from the same day of the week before and the week after, if possible. If one (or both) of those days were missing, then two or more weeks before or after were used. Speed and lateral position data were not interpolated.

Data acquisition and analysis for the Highway 59 Research Project are described in this chapter. Some data calculations, such as speed, axle spacing, and weight, were done on-site with the PAT software and could be viewed in real time on a computer screen. The weight, lateral position, and temperature measurements were calibrated and the pavement roughness measured. Calibrations, particularly of the weighpad signals, should be performed on a periodic basis. Additional data analysis was done with an Excel macro after the data files were transferred to Austin. Results from the data analysis will be discussed in the following four chapters.

Chapter 5 Volume and Speed

In this chapter, the results of the data analysis described in the previous chapter are discussed. Different methods of classifying vehicles based on the number of axles and the axle spacing will be discussed in the first section and the volume and speed statistics will be described. Periodic trends of traffic volume and speed by day of the week and month of the year will be discussed in the second section.

5.1 Vehicle Classification

To study the effects of traffic loading on pavement performance it was necessary to be able to estimate the number and types of vehicles crossing a given point. Various criteria were used to classify vehicles, including overall length, wheelbase, number of axles, spacing between axles, presence of dual tires, number of trailers, or combinations of these criteria.

The Federal Highway Administration (FHWA) has established a thirteen-class vehicle sorting system that is based on the number of axles per vehicle and whether trucks are single-unit, single-trailer, or multitrailer, as shown in Table 5.1 (Traffic Monitoring Guide 1995). The first four categories are for nontruck vehicles, namely, motorcycles, passenger cars, buses, and other two-axle vehicles (pickup trucks and vans). Passenger cars and pickup trucks pulling trailers are included in class two and three instead of the three-axle or four-axle classes. If the only data available are the number of axles and the spacing between axles, it is difficult if not impossible to distinguish between some classes, for example between passenger cars and pickup trucks or between buses and single-unit trucks. Another classification method proposed by the American Society for Testing and Materials (ASTM) and shown in Table 5.2 uses only the number of axles and the spacing between axles (Standard Specification E 1318-94 1996). The first digit of the vehicle code is the number of axles while the second digit depends on the axle spacing pattern. One of the simplest ways to classify vehicles is by the number of axles, which was the method used on the data from the Highway 59 Research Project. After vehicles have been sorted by this scheme, they can be further subdivided into more categories depending on such criteria as the spacing between axles, number of axles with dual tires, weight of wheels, axles, or axle groups, or gross vehicle weight. Initially, the vehicles were sorted into the two-axle class, which was the largest class in terms of number, and the three-or-more axle class. Later this class was

further sorted into three-, four-, five-, and six-or-more axle classes. Of these, the five-axle vehicle class was the largest. Both the two-axle and five-axle classes may be further subdivided into additional classes, based on additional criteria.

Table 5.1 FHWA Vehicle Classes (Traffic Monitoring Guide 1995)

Class	Description
1	Motorcycles
2	Passenger Cars
3	Other Two-Axle, Four-Tire, Single-Unit Vehicles
4	Buses
5	Two-Axle, Six-Tire, Single-Unit Trucks
6	Three-Axle, Single-Unit Trucks
7	Four-or-More Axle, Single-Unit Trucks
8	Four-or-Less Axle, Single-Trailer Trucks
9	Five-Axle, Single-Trailer Trucks
10	Six-or-More Axle, Single-Trailer Trucks
11	Five-or-Less Axle, Multitrailer Trucks
12	Six-Axle, Multitrailer Trucks
13	Seven-or-More Axle, Multitrailer Trucks

Table 5.2 ASTM Vehicle Classes (Standard Specification E 1318-94 1996)

Range of Spacing Between Axle Pairs, ft 1 ft = 0.3048 m					
Class	A,B	B,C	C,D	D,E	E,F
21	6-9				
22	9-11				
23	11-25				
20	other				
31	8-26	2-6			

Range of Spacing Between Axle Pairs, ft 1 ft = 0.3048 m					
Class	A,B	B,C	C,D	D,E	E,F
32	8–20	11–45			
33	8–10	6–22			
30	other				
41	8–20	11–45	2–6		
42	8–20	2–6	11–45		
43	8–20	2–6	2–6		
40	other				
51	8–25	2–6	11–55	2–6	
52	8–20	11–36	6–20	7–35	
50	other				
61	8–20	2–6	11–42	2–6	2–6
62	8–20	2–6	11–30	7–15	11–25
60	other				

The percentage of each vehicle class in each lane at each site is shown in Table 5.3. The two-axle class, which includes passenger cars, pickup trucks, vans, and some single-unit trucks, accounted for 75 percent of all vehicles in the right lane and nearly 90 percent of all vehicles in the left lane. There was little difference between sites in the proportions of vehicle classes making up the total volume.

Table 5.3 Percentage of Volume by Vehicle Class

Vehicle Class	North Site		South Site	
	Right Lane	Left Lane	Right Lane	Left Lane
Two Axle	75.7%	88.7%	75.2%	89.3%
Three Axle	2.6%	1.8%	2.6%	1.8%
Four Axle	2.5%	1.6%	2.9%	1.5%
Five Axle	18.8%	7.7%	18.9%	7.1%
Six-or-More Axle	0.4%	0.2%	0.5%	0.3%

The statistics for speed and volume for 1993 are shown in Table 5.4 for both the north and the south site. The right lane at the north site had a 6.6 percent higher volume than the right lane at the south site, while the left lane at the south site had a 9.3 percent higher volume than the left lane at the north site. The total volume was 2 percent higher at the north site. The volume of five-axle vehicles was 4.5 percent higher, while the volume of two-axle vehicles was 1.5 percent higher. The Highway 287 intersection in Corrigan may have accounted for some of the difference, while local lumber operations may also have accounted for some of the difference. The left lane had 24.8 percent of the total volume at the north site and 27.9 percent of the total volume at the south site. The average speeds were somewhat higher in the left lane than in the right lane at each site. The average speeds were somewhat higher at the north site than at the south site. The north site was located at the end of a downgrade while the south site was at the beginning of a downgrade. The south site was about 2 miles downstream from a traffic signal and about a mile downstream from a reduced speed zone, so the traffic was not as dispersed as that at the north site. The traffic light and reduced speed zone may also have accounted for the difference in lane distribution between sites. The standard deviation of the speed was significantly lower for the right lane at the north site, possibly because vehicles in the left lane and at the south site were less independent of other vehicles owing to the effect of the speed zone at the south site, and the fact that left-lane vehicles were more likely to be passing right-lane vehicles.

Table 5.4 Volume and Speed Statistics for 1993

1 mi/h = 1.609 km/h

		Right Lane		Left Lane	
		Volume veh. per day	Speed mi/h	Volume veh. per day	Speed mi/h
North	Mean	5,336 (75.2%)	65.8	1,760 (24.8%)	69.2
	Minimum	3,120	63.3	1,026	62.9
	Maximum	9,424	66.8	5,906	71.9
	St Dev	719	0.5	553	1.1
	Total	1 947 812		642 426	
South	Mean	5,012 (72.1%)	63.3	1,941 (27.9%)	65.9
	Minimum	2,472	60.9	1,056	59.3
	Maximum	8,795	65.8	6,855	69.9
	St Dev	671	1.2	639	1.3
	Total	1 829 519		708 386	

Table 5.5 shows the average speed of each vehicle class for each location. The left lanes at each site had higher average speeds than the respective right lanes. The north site had higher average speeds than the south site. The five-axle vehicle class had the highest average speeds for all cases. The six-or-more-axle class had the lowest average speeds for the left lanes, while the four-axle class had the lowest average speeds for the right lanes.

Table 5.5 Average Speed by Vehicle Class, mi/h

1 mi/h = 1.609 km/h

	North Site		South Site	
	Right Lane	Left Lane	Right Lane	Left Lane
All vehicles	66	69	63	66
2-axle Vehicles	65	69	63	66
3-axle Vehicles	66	70	63	66
4-axle Vehicles	64	69	61	65
5-axle Vehicles	68	72	64	67
6-or-more-axle Vehicles	67	68	62	64

In this section, two methods used by the FHWA and ASTM to classify vehicles are presented. A simplified method based on the number of axles per vehicle was used for the Highway 59 Research Project. The statistics tables show that 75 percent of vehicles traveled in the right lane, and 75 percent of right-lane vehicles were in the two-axle class. In the left-lane 90 percent of vehicles were two-axle vehicles. An average of 7,000 vehicles passed each day with an average speed ranging from 98 km/h to 115 km/h (62 to 72 mi/h) depending on class and location. The five-axle vehicles had the highest average speeds. The posted speed limit in 1993 was 88 km/h (55 mi/h).

5.2 Periodic Trends

This section will discuss the average speed trends and the average daily volume trends by day of the week and by month.

Table 5.6 shows the average speed by day of the week. On Sundays the average speed was faster by 1.6 km/h (1 mi/h) in each location except the right lane at the north site.

The average speed for the left lane at the south site was 1.6 km/h (1 mi/h) slower on Tuesdays, and the right-lane speed at the north site was 1.6 km/h (1 mi/h) slower on Saturdays.

Table 5.6 Average Speed by Day of the Week, mi/h

1 mi/h = 1.6 km/h

	North Site		South Site	
	Right Lane	Left Lane	Right Lane	Left Lane
Sunday	66	70	64	67
Monday	66	69	63	66
Tuesday	66	69	63	65
Wednesday	66	69	63	66
Thursday	66	69	63	66
Friday	66	69	63	66
Saturday	65	69	63	66

Table 5.7 shows the average speed at each location for each month. Average speeds at the south site gradually increased throughout the year from 100 km/h to 105 km/h (62 mi/h to 65 mi/h) in the right lane and from 105 km/h to 108 km/h (65 mi/h to 67 mi/h) in the left lane. Average speeds at the north site showed only slight fluctuations.

Table 5.7 Average Speed by Month, mi/h

1 mi/h = 1.609 km/h

	North Site		South Site	
	Right Lane	Left Lane	Right Lane	Left Lane
January	65	69	62	65
February	66	69	62	65
March	66	70	62	65
April	66	69	63	65
May	66	70	62	65
June	66	69	62	65
July	66	69	63	66
August	66	70	64	66
September	66	69	64	66
October	66	69	64	67
November	66	69	64	67
December	66	69	65	67

Figures 5.1 through 5.4 show the average daily volume by day of the week at each site for each lane for two-axle vehicles, five-axle vehicles, and total vehicles. Other classes of vehicles are not included on the graphs because of their comparatively small volumes. Sunday was the highest volume day for two-axle vehicles while it was the second lowest day after Saturday for five-axle vehicles. The two highest volume days were 28 November and 26 December, the Sundays following Thanksgiving and Christmas. Sundays were the highest volume days followed by Fridays. Tuesdays and Wednesdays were the lowest volume days. Saturday was the only day of the week where the south site had a higher volume of vehicles than the north site. On Mondays, the volume difference between sites was greatest, while on Sundays the volume difference was least.

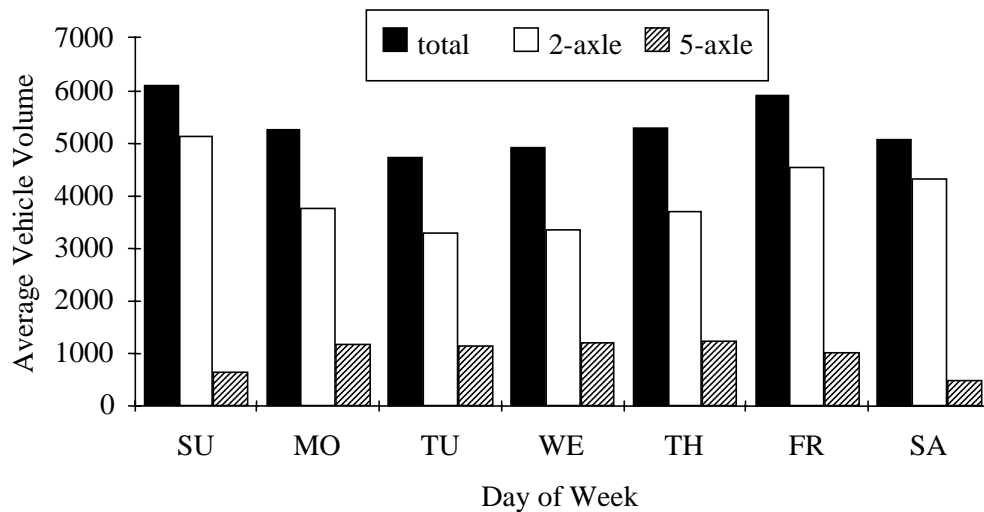


Figure 5.1 Average Daily Volume by Day of Week, North Site, Right Lane

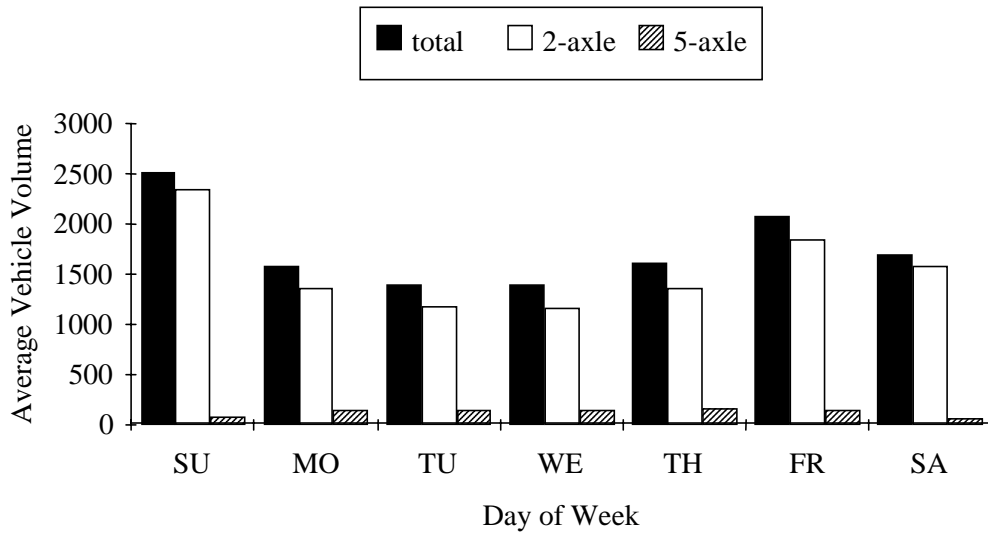


Figure 5.2 Average Daily Volume by Day of Week, North Site, Left Lane

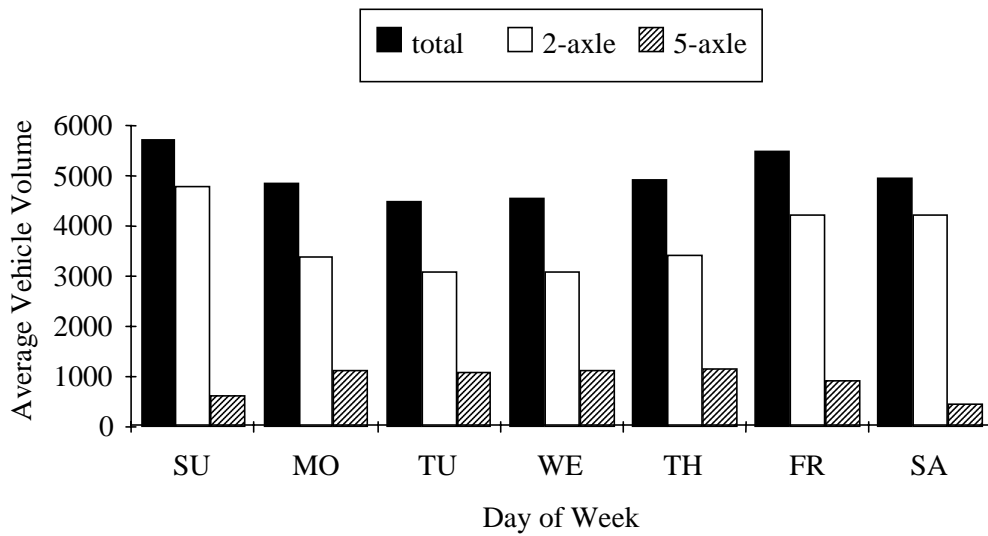


Figure 5.3 Average Daily Volume by Day of Week, South Site, Right Lane

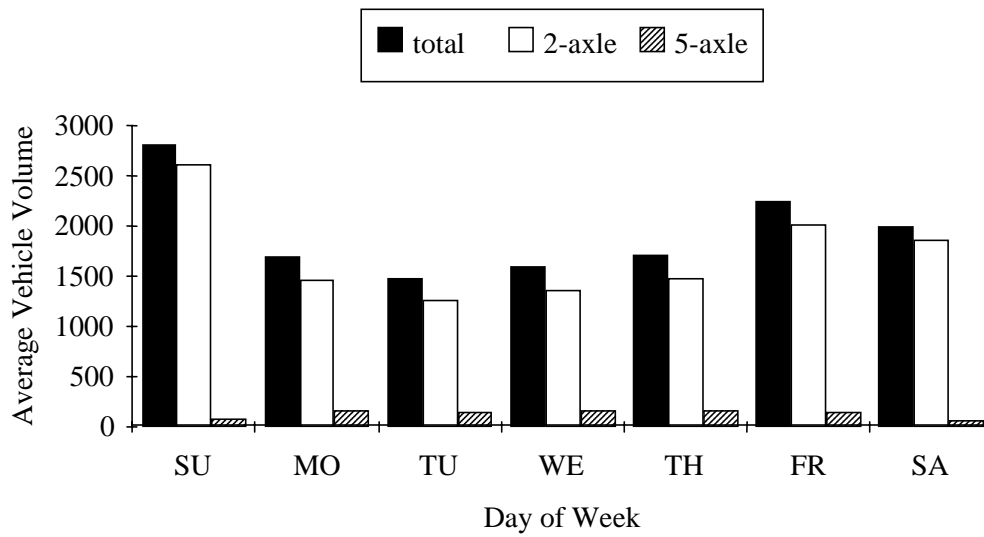


Figure 5.4 Average Daily Volume by Day of Week, South Site, Left Lane

Figures 5.5 through 5.8 show the average daily volume by month at each location for the two-axle and five-axle vehicle classes and for all vehicles. Other vehicle classes are not shown in the graphs because of their comparatively small volumes. In each case, January was the month with the lowest average daily traffic. The traffic volume increased each month until it peaked in July, then decreased until September, and then increased again to the end of the year. For the right lane at both the north and south sites, the July peak was higher, while in the left lane at both sites, the November peak was higher. The five-axle vehicle volume did not vary as much as the two-axle vehicle volume. The two highest volume days of the year occurred in November and December on the Sundays following Thanksgiving and Christmas. Other days near these holidays also had high traffic volumes though Thanksgiving Day and Christmas Day had relatively low traffic volumes.

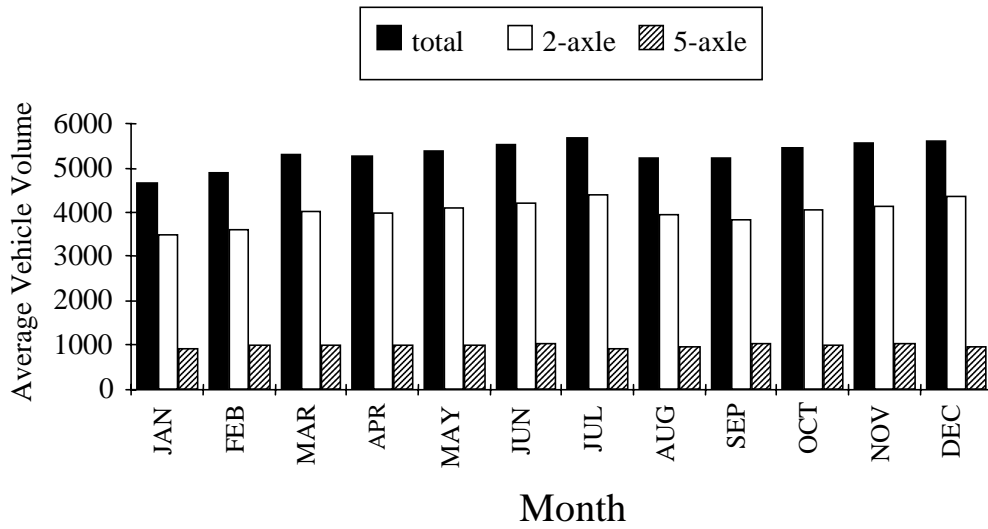


Figure 5.5 Average Daily Volume by Month, North Site, Right Lane

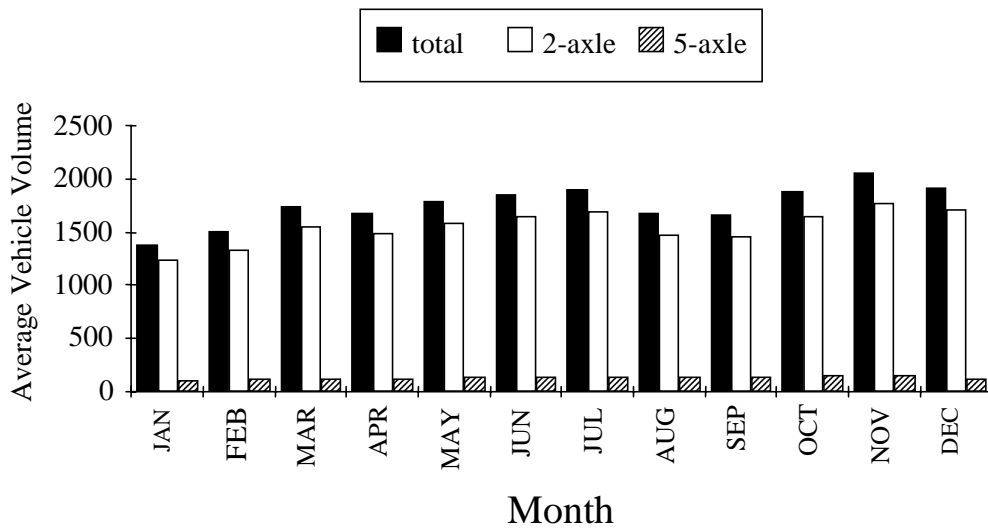


Figure 5.6 Average Daily Volume by Month, North Site, Left Lane

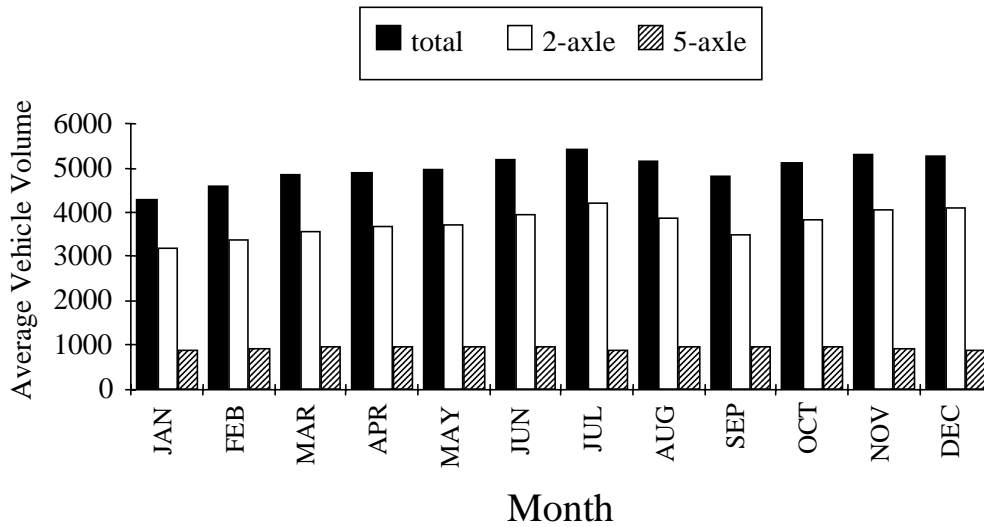


Figure 5.7 Average Daily Volume by Month, South Site, Right Lane

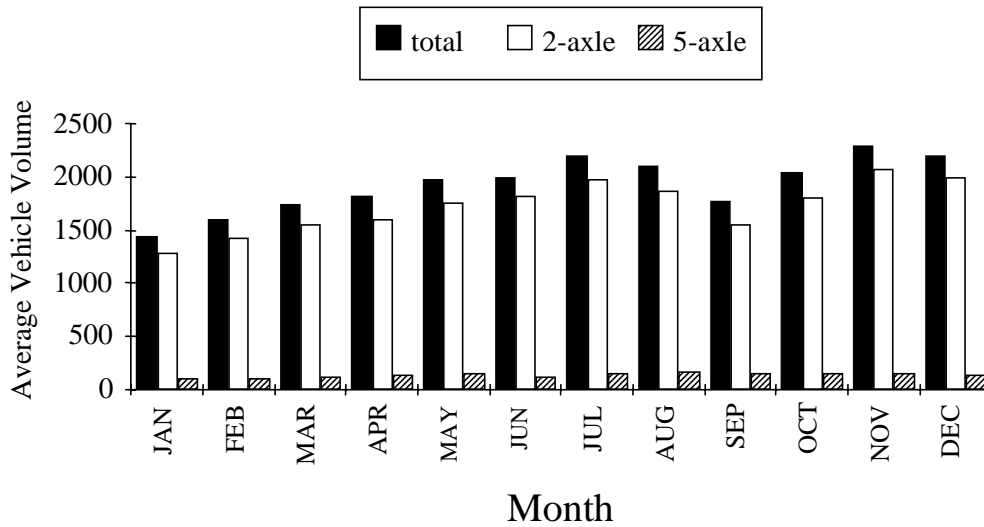


Figure 5.8 Average Daily Volume by Month, South Site, Left Lane

Of the various ways to classify vehicles, the number of axles per vehicle was used for simplicity. There were a few minor differences in traffic volume and speed patterns between the north and south sites. Some of these differences were because vehicles exit or enter the highway at the intersection in Corrigan. The traffic light in Corrigan also caused downstream

vehicles to be less dispersed. The speed data varied only slightly by day of the week and by month, though the speeds at the south site increased gradually throughout the year. The average speed varied between classes and between lanes. Weekend and weekday traffic volumes were different as expected, with more passenger cars and fewer trucks on the weekends. Holiday travel patterns also accounted for much variability. The Sundays following Thanksgiving and Christmas were the two days with the highest volume of traffic. The Labor Day holiday and Memorial Day weekends also had significantly higher traffic volume. The 1993 data should be compared with data from subsequent years to examine seasonal trends and annual growth rates.

Chapter 6 Axle Loads and ESALs

The repeated dynamic forces of heavy vehicle tires on highway pavements are the major cause of pavement damage. These forces can be measured with weigh-in-motion (WIM) equipment and used to estimate the corresponding tire loads of static vehicles. The sum of the tire loads on all wheels of the same axle is called axle load (the portion of the gross vehicle weight supported by the axle) and the sum of all axle loads on the static vehicle is the gross vehicle weight. Gross vehicle weight is the force due only to the local force of gravity acting vertically downward upon the composite mass of the static vehicle with a magnitude equal to the product of vehicle mass, kg or lb (avoirdupois), and the local acceleration of free fall, nominally 9.81 m/s^2 or 32.17 ft/s^2 , though this value differs slightly at various localities on Earth. For scientific and technical use, weight should be expressed in force units. In the SI system of units, force is expressed in terms of the newton, N, i.e., the force that, when applied to a body having a mass of one kilogram, results in an acceleration of 1 meter per second squared. However, for weighing highway vehicles, all vehicle scales (required for single-draft, commercial weighing), axle-load scales, portable axle-load weighers, and wheel-load weighers are adjusted to indicate units of mass, kg or lb (avoirdupois), at the locality of use. Therefore, in commercial and everyday use by scale operators, shippers, truckers, lawmakers, and enforcement personnel, the terms weight and load are usually synonymous with mass. Such is the case in this report. To convert indicated mass, e.g., kg, to force units, i.e., $\text{kg}\cdot\text{m/s}^2$, mass must be multiplied by the local acceleration of free fall. In the SI system of units, the base unit of mass is the kilogram, kg. SI prefixes are used to express multiples of units. For expressing axle load and gross vehicle weight (large masses), it is convenient to use the prefix mega, M, to modify gram, g. One Mg equals 1,000 kg. (Note: The metric ton of 1,000 kg, is not an SI term.) In the U.S. customary system of units, one kip equals 1,000 lb (avoirdupois). To convert kip to Mg, multiply by 0.4536.

Experience at the AASHO Road Test demonstrated that pavement damage resulting from truck traffic is nonlinear with respect to the number of applied axle loads, as discussed in Chapter 2. To normalize the effects of different axle types (single, tandem) and magnitudes of axle loads, researchers derived the concept of the equivalent single axle load (ESAL) factor from analysis of the AASHO Road Test data. Axle loads of the AASHO Road Test trucks were measured with the vehicles static and reported in mass units, lb

(avoirdupois). The number of applications of a standard, e.g., 8.2 Mg (18-kip), single (dual-tire) axle load that will cause the same damage to a given pavement structure as one application of a given axle load on a defined axle type is called an ESAL factor. The cumulative number of ESALs observed or estimated within a defined time period are referred to as ESALs. In the following sections, the process of calculating ESALs from observed wheel-load data sets is illustrated, periodic trends in axle loads and ESALs are shown, and an algorithm for predicting ESALs from traffic-count and classification data is presented.

6.1 Equivalent Single Axle Load Calculations

To normalize the effects of mixed traffic loading to a single number, ESAL factors were used. The formulas are based on the results of the AASHO Road Test, which were discussed in Chapter 2 (HRB Special Report 61A 1961; HRB Special Report 61E 1962; Carey and Irick 1962; ASTM Standard Specification E 1318-94 1996; Leidy 1994). The calculations were carried out by the Excel macro described in Chapter 4.

Flexible pavement equivalence factors are also used for composite pavements, or for flexible overlays placed on top of rigid pavements.

The AASHO design equations for flexible pavements are:

$$\log W_t = 5.93 + 9.36 \log(\overline{SN} + 1) - 4.79 \log(L_1 + L_2) + 4.33 \log L_2 + \frac{G_t}{\beta}$$

$$\beta = 0.40 + \frac{0.081(L_1 + L_2)^{3.23}}{(\overline{SN} + 1)^{5.19} L_2^{3.23}}$$

$$G_t = \log \left[\frac{4.2 - P_t}{4.2 - 1.5} \right]$$

The variables are defined as follows:

W_t = number of axle load applications at end of time t for axle sets with dual tires

\overline{SN} = structural number; determined from the thickness, in inches, and stiffness of pavement layers

L_1 = load on single axle, tandem axle set, or tridem axle set, in kip

L_2 = axle code (one for single axle, two for tandem axles, three for tridem axles)

P_t = pavement serviceability at end of time t ; terminal serviceability is determined from the desired quality of the pavement at the time of future overlay and is commonly taken as 2.5.

β = shape function

G_t = logarithm of ratio of loss in serviceability at time t to the potential loss at time when $P_t = 1.5$

The equation for calculating ESAL factors for flexible pavements is:

$$E_i = \frac{W_{t_{18}}}{W_{t_i}} = \left[\frac{(L_i + L_2)^{4.79}}{(18+1)^{4.79}} \right] \left[\frac{10^{G_t/\beta_{18}}}{(10^{G_t/\beta_i}) L_2^{4.33}} \right]$$

E_i = equivalence factor; number of 18-kip single-axle load applications, $W_{t_{18}}$, needed to cause damage to a given pavement structure equivalent to one application, W_{t_i} , of the given axle load, L_i .

Rigid pavement equivalence factors have a format similar to the flexible pavement equations, except that slab thickness, in inches, is used instead of the structural number (SN).

The AASHO design equations for rigid pavements are:

$$\log W_t = 5.85 + 7.35 \log(D+1) - 4.62 \log(L_1 + L_2) + 3.28 \log L_2 + \frac{G_t}{\beta}$$

$$\beta = 1.0 + \frac{3.63(L_1 + L_2)^{5.20}}{(D+1)^{8.46} L_2^{3.52}}$$

$$G_i = \log \left[\frac{4.5 - P_i}{4.5 - 1.5} \right]$$

D = thickness of rigid pavement slab in inches

The other variables are the same as for flexible pavements.

The equivalence factor for rigid pavements is:

$$E_i = \frac{W_{i18}}{W_i} = \left[\frac{(L_i + L_2)^{4.62}}{(18 + 1)^{4.62}} \right] \left[\frac{10^{G_i / \beta_{18}}}{(10^{G_i / \beta_i}) L_2^{3.28}} \right]$$

The equivalence factor is a function of axle load, axle type, SN or slab thickness, and terminal serviceability. These equations are units sensitive; kip must be used for axle load and inch for pavement thickness.

For the Highway 59 project, the terminal serviceability was fixed at 2.5. The SN varied from 6 to 8 for the south test sections, and from 4 to 11 for the north test sections. The south test sections were originally flexible, while the north test sections were originally rigid before being overlaid with asphalt concrete periodically as they became rough. All test sections received an asphalt overlay as the final stage in the reconstruction process. ESAL equations for flexible pavements were used for the originally rigid test sections as the surface course was asphalt along with many of the lower layers. SNs greater than 6 did not noticeably change the results of the calculated equivalence factors. At the AASHO Road Test the SNs ranged from 1 to 6.

The AASHTO Guide recommends that for tridem axle calculations the number 3 be used for the axle code variable L_2 (AASHTO Guide, Vol. 2, Appendix MM, 1988). Only single and tandem axles were used in the original AASHO Road Test. There is considerable uncertainty in extending the equations to tridem axles. Separate studies have been conducted for both rigid and flexible pavements. These indicate that the AASHTO recommendations are reasonable and possibly overly conservative.

Axles that have single tires cause more damage than axles with the same load but with dual tires. Table 6.1 shows comparisons between single axles with single tires and with

dual tires (Lee, Shankar, and Izadmehr 1983). Although the steering axles used in the AASHO Road Test had single tires, the data were not considered separately from the other axles with dual tires. Rather, the equivalent damage factor for steering axles was incorporated into the equivalent damage factor for other axle groups on the vehicle. The loads on the steering axles at the road test ranged from 0.9 to 5.4 Mg (2 to 12 kip). For steering axles greater than 5.4 Mg (12 kip), separate ESAL calculations are required. Because axle loads less than 0.9 Mg (2 kip) were not used in the AASHO Road Test, the formulas described above are not strictly applicable to passenger cars. However, most analyses have indicated that the total ESALs and the associated pavement damage caused by passenger cars is negligible in comparison to that produced by trucks.

The average steering-axle load for five-axle vehicles is about 4.5 Mg (10 kip), and about 1 percent of steering-axle loads are over 5.4 Mg (12 kip). The values from Table 6.1 may be used to estimate the equivalent damage factors for steering-axle loads over 5.4 Mg (12 kip).

**Table 6.1 Steering Axle (Single Tire) ESAL Comparisons
(Lee, Shankar, and Izadmehr 1983)**

		Single Tires	Dual Tires
kip	Mg	ESALs	ESALs
12	5.44	0.62	0.176
14	6.35	0.93	0.342
16	7.26	1.33	0.606
18	8.16	1.90	1.00
20	9.07	2.44	1.55
22	9.98	3.15	2.30
24	10.9	3.95	3.27
26	11.8	4.82	4.48
28	12.7	5.83	5.98
30	13.6	6.80	7.8

Axle spacings are needed to determine whether axles are single, tandem, or tridem. An axle spacing less than 1.8 m (6 ft) indicates a tandem axle set. If the sum of two

successive axle spacings is less than 3.7 m (12 ft), then a tridem axle set is indicated. All the front axles are assumed to be steering axles with single tires, and equivalence factors should not be applied unless the steering-axle load is over 5.4 Mg (12 kip). For two-axle vehicles, the second axle is assumed to be single with dual tires, and the equivalence factors can be calculated in one step. For vehicles with more than two axles, a determination has to be made for each vehicle of whether every axle except the front axle is single or part of a tandem or tridem axle set. Therefore, the equivalence factors for all axles except the steering axle are calculated individually for every vehicle with more than two axles.

The AASHO Road Test considered only SNs up to 6; currently many highway pavements are designed with SNs of 9 or higher. The effect of SN on the equivalence factors is erratic and not completely consistent with theory. With heavy axle loads and ESALs much greater than unity, the equivalence factor increases as SN decreases, which is as expected because heavy axle loads are more destructive to weaker pavements. In the ESAL equations, higher SNs may be used; however, the resulting equivalence factors are almost unchanged from the SN 6 equivalence factors (Huang 1993).

The ESAL concept is used to normalize the damaging effects of mixed traffic loading. The variables used in the calculation include axle load; indication of steering, single, tandem, or tridem axles; SN, which indicates the depth and stiffness of the pavement; and the terminal serviceability, which indicates the desired quality of the pavement at the time of future overlay. Equivalence factors for steering-axle loads heavier than 5.4 Mg (12 kip) should be calculated separately.

6.2 Periodic Trends

In this section, the trends of observed axle loads and ESALs on a daily and monthly basis are discussed. The differences between the north and south sites, between the right and left lanes, and between vehicle classes are described.

The daily axle loads and ESAL statistics for both the north and south sites are shown in Table 6.2. The minimum values for axle loads and ESALs at the north site all occurred on 25 December, Christmas Day. The maximum values for axle loads and ESALs at the north site occurred on 20 and 27 May, for the right lane, and 2 November for the left lane. The

minimum values for axle loads and ESALs at the south site occurred on 1 January and 25 December. The maximum values for axle loads and ESALs at the south site occurred on 19, 20, and 27 May. The right lane at the north site had 6.8 percent heavier axle loads and 13 percent more ESALs than the right lane at the south site, while the left lane at the north site had 1.4 percent lighter axle loads but 19 percent more ESALs than the left lane at the south site. The north site had greater variability in loads than the south site. The right lane at the north site had 84 percent of the total axle loads and 87 percent of the total ESALs. The right lane at the south site had 83 percent of the total axle loads and 88 percent of the total ESALs. In the right lanes, the ratio of axle loads to ESALs was 23 Mg (50 kip) per ESAL at the north and 25 Mg (54 kip) per ESAL at the south. The ratio for the left lanes was quite a bit higher, 30 Mg (66 kip) per ESAL at the north site and 38 Mg (83 kip) per ESAL at the south site. This was probably because the heavier vehicle classes traveled more in the right lane than the left. Another reason for the difference between lane loading was that vehicles with overweight permit loads, which contribute disproportionately to the ESAL totals, tended to travel at lower speeds and would thus more likely be in the right lanes.

Table 6.2 Daily Axle Loads and ESAL Statistics by Lane

1 kip = 0.4536 Mg

	Right		Left	
	Mg	ESAL	Mg	ESAL
North				
Total	13 849 875	607 440	2 647 131	88 099
Mean	37 945	1 664	7 252	241
Minimum	10 137	110	3 270	32
Maximum	50 976	2 653	23 846	1 156
St Dev	8 309	551	1 968	108
South				
Total	12 912 309	526 548	2 685 539	71 034
Mean	35 376	1 443	7 358	195
Minimum	10 061	108	3 369	27
Maximum	47 538	2 356	19 885	771
St Dev	7 693	488	1 774	77

The axle-load and ESAL statistics by day of the week are shown in Table 6.3. The lowest values for average axle loads and ESALs for all lanes occurred on Saturdays. The highest values for average axle loads and ESALs for the right lanes at each site occurred on

Thursdays. The highest average values for axle loads in the left lanes at both sites occurred on Fridays. The highest average number of ESALs in the left lanes occurred on Wednesdays at the south site and on Thursdays at the north site. The axle load to ESAL ratio was quite a bit higher on weekends than on weekdays. For Monday through Thursday the average ratios were 21 Mg (47 kip) per ESAL north site, right lane; 23 Mg (51 kip) south site, right lane; 26 Mg (58 kip) north site, left lane; and 33 Mg (72 kip) south site, left lane. On Saturday the respective ratios jumped to 29, 32, 43, and 59 Mg (65, 70, 94, and 130 kip) per ESAL.

Table 6.3 Average Total Axle Loads and ESALs by Day of the Week

		Right			Left		
		Kip	Mg	ESAL	Kip	Mg	ESAL
North	Sun	67 830	30 768	1 113	16 659	7 557	174
	Mon	95 615	43 371	2 025	16 602	7 531	281
	Tue	88 523	40 154	1 846	15 861	7 194	279
	Wed	95 385	43 267	2 035	15 712	7 127	271
	Thu	99 274	45 031	2 103	17 517	7 946	302
	Fri	87 633	39 750	1 736	18 035	8 181	261
	Sat	51 231	23 238	789	11 496	5 215	122
South	Sun	62 876	28 521	972	17 523	7 948	145
	Mon	89 766	40 718	1 776	16 809	7 625	235
	Tue	84 745	38 440	1 662	15 010	6 809	208
	Wed	88 228	40 020	1 732	16 800	7 620	237
	Thu	91 678	41 585	1 792	16 987	7 705	235
	Fri	80 231	36 393	1 470	17 940	8 138	205
	Sat	48 361	21 937	694	12 442	5 644	96

The average total daily axle loads by day of the week for each location are shown in Figures 6.1 through 6.4. In the right lanes, the average value was less on Saturdays and Sundays than on weekdays, while in the left lanes, only the Saturday value was lower than other days. Two-axle vehicles contributed a greater proportion of the total axle loads in the

left lanes than in the right lanes. On weekends, the two-axle vehicles contributed the majority of the total loads.

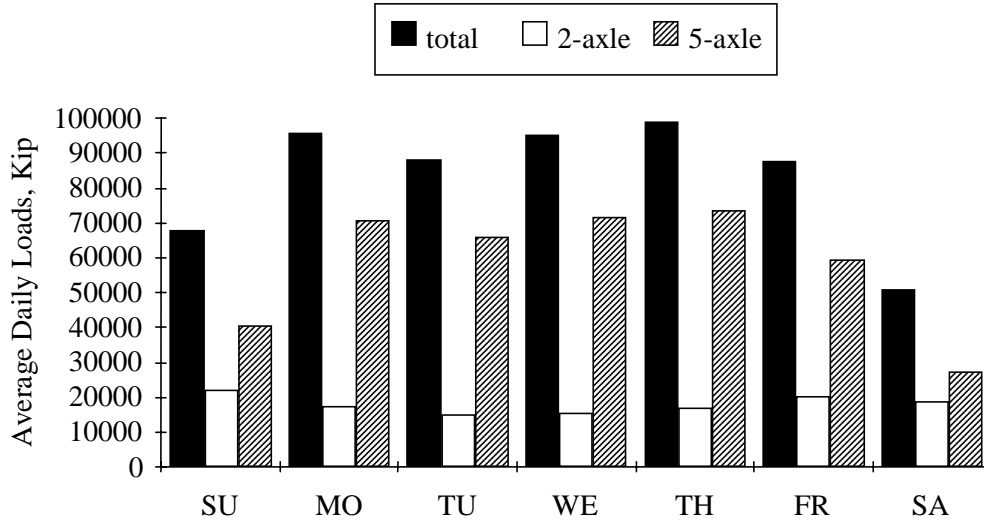


Figure 6.1 Axle Load by Day of Week, North Site, Right Lane

1 kip = 0.4536 Mg

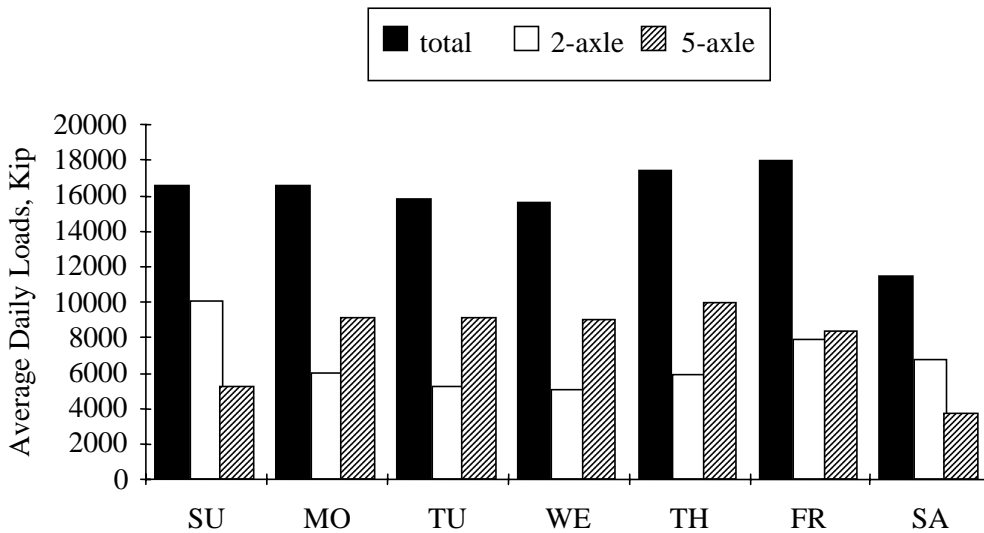


Figure 6.2 Axle Load by Day of Week, North Site, Left Lane

1 kip = 0.4536 Mg

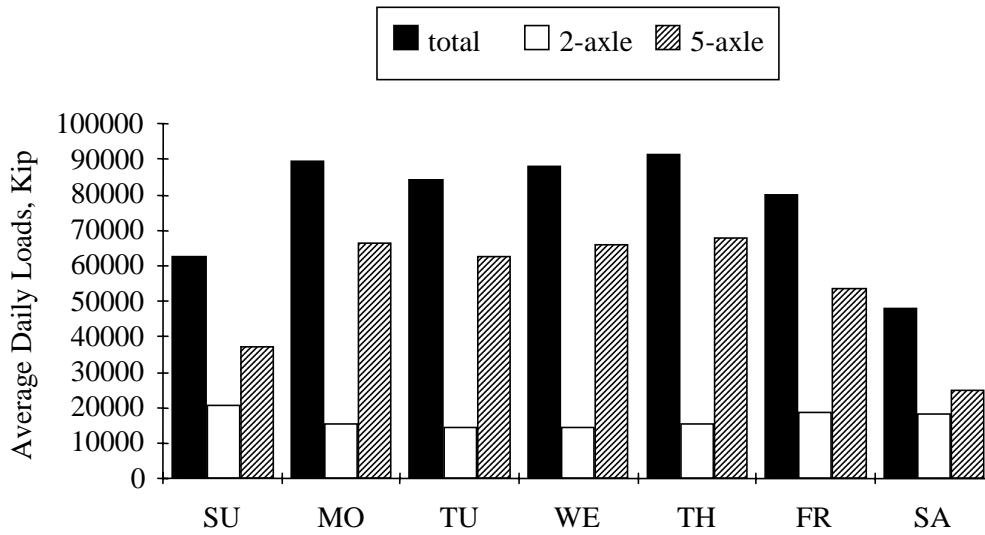


Figure 6.3 Axle Loads by Day of Week, South Site, Right Lane
1 kip = 0.4536 Mg

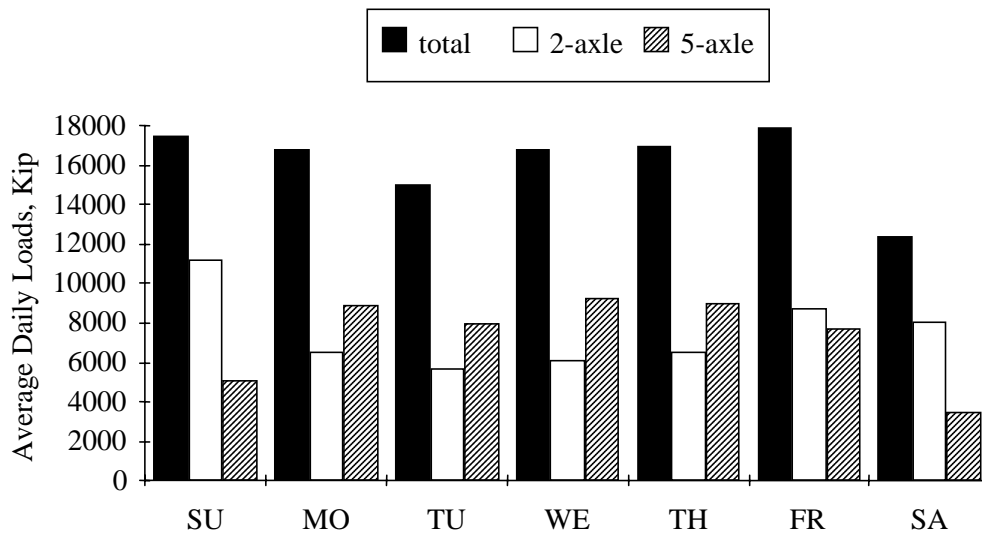


Figure 6.4 Axle Loads by Day of Week, South Site, Left Lane
1 kip = 0.4536 Mg

Figures 6.5 through 6.8 show the average total daily axle loads for each month in 1993. The loads of the two-axle and five-axle classes and the total loads are shown for each lane at both sites. January and other winter months had lower values, while June and other

summer months had higher values. In the left lanes, the proportion of total axle loads owing to two-axle vehicles was often higher than that for the five-axle class.

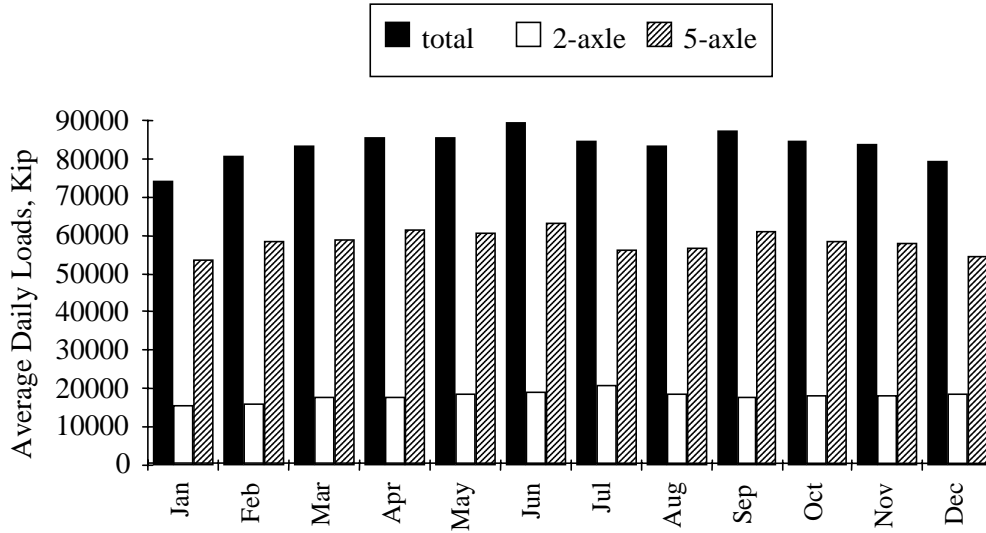


Figure 6.5 Axle Loads by Month, North Site, Right Lane

1 kip = 0.4536 Mg

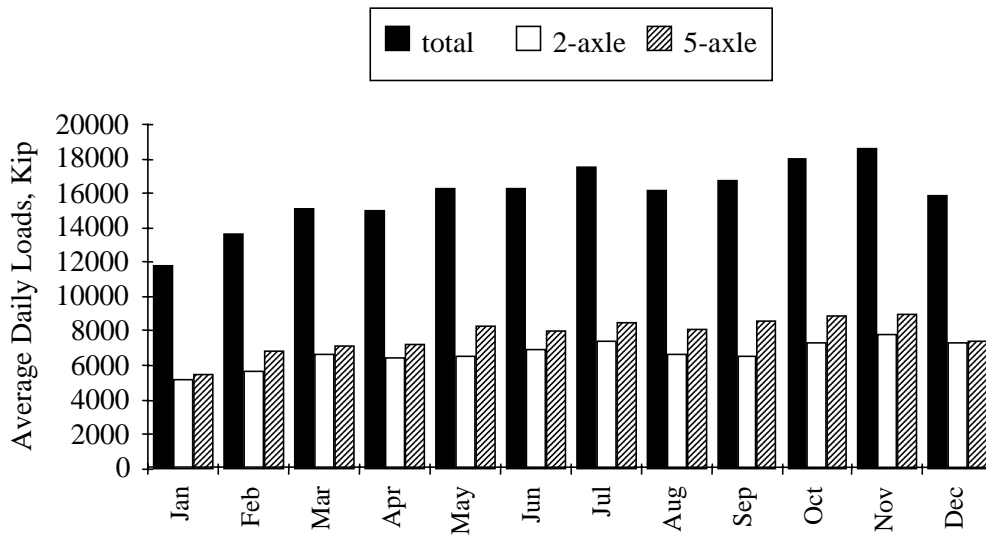


Figure 6.6 Axle Load by Month, North Site, Left Lane

1 kip = 0.4536 Mg

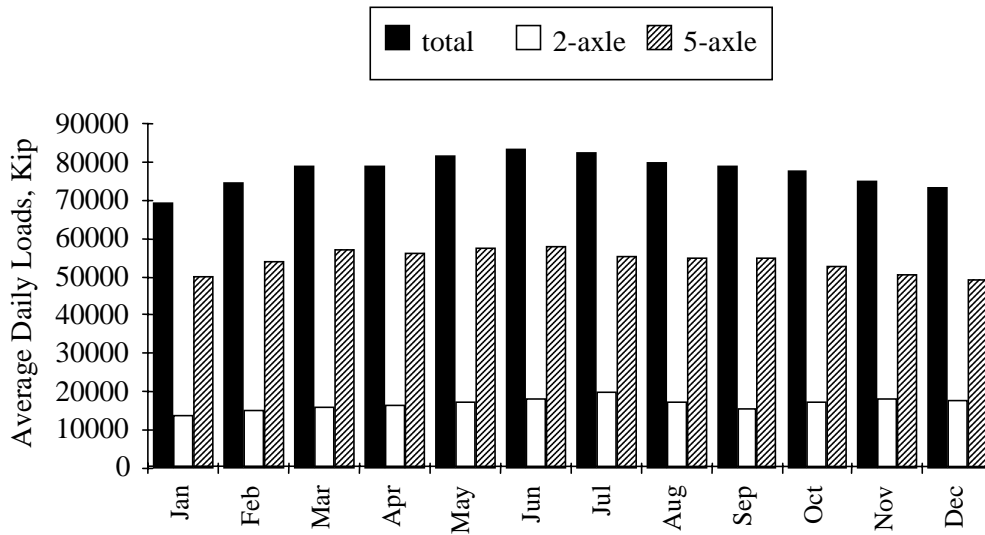


Figure 6.7 Axle Load by Month, South Site, Right Lane
 1 kip = 0.4536 Mg

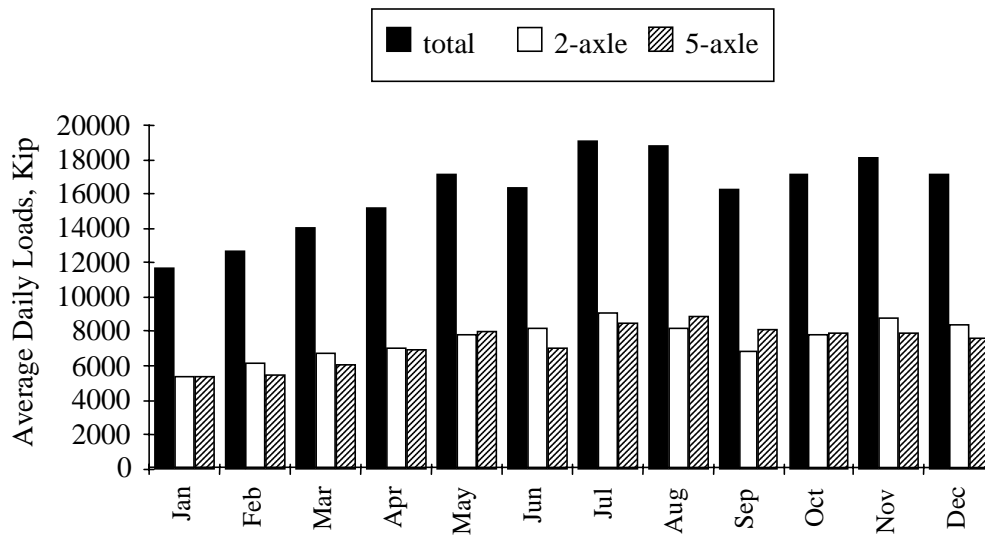


Figure 6.8 Axle Load by Month, South Site, Left Lane
 1 kip = 0.4536 Mg

Figures 6.9 through 6.12 show the average daily ESALs for each location by day of the week. Saturday was the day with the lowest average number of ESALs followed by Sunday; the day with the highest average number of ESALs was Thursday, followed by

Monday. This followed the pattern of five-axle vehicles, which contributed the majority of all ESALs. The contribution of two-axle vehicles was negligible in the right lanes.

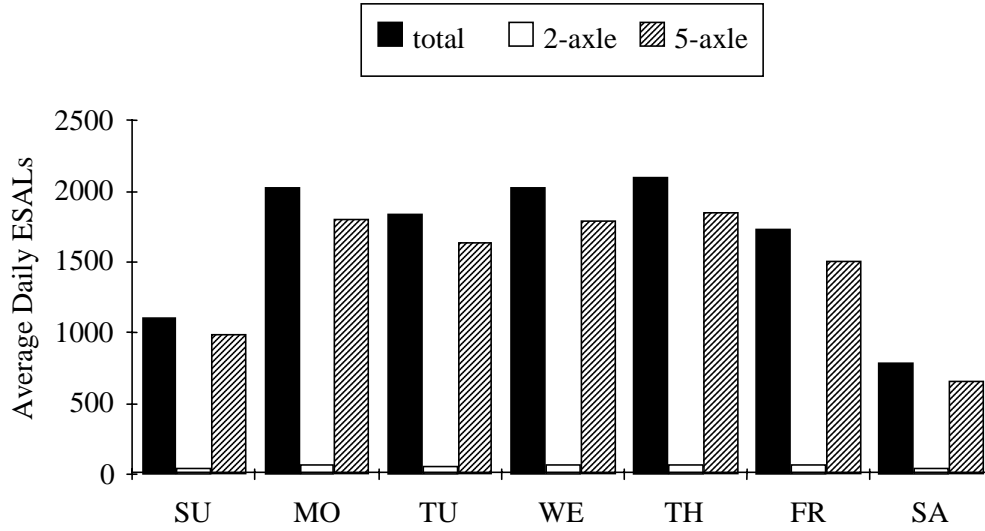


Figure 6.9 Average ESALs by Day of Week, North Site, Right Lane

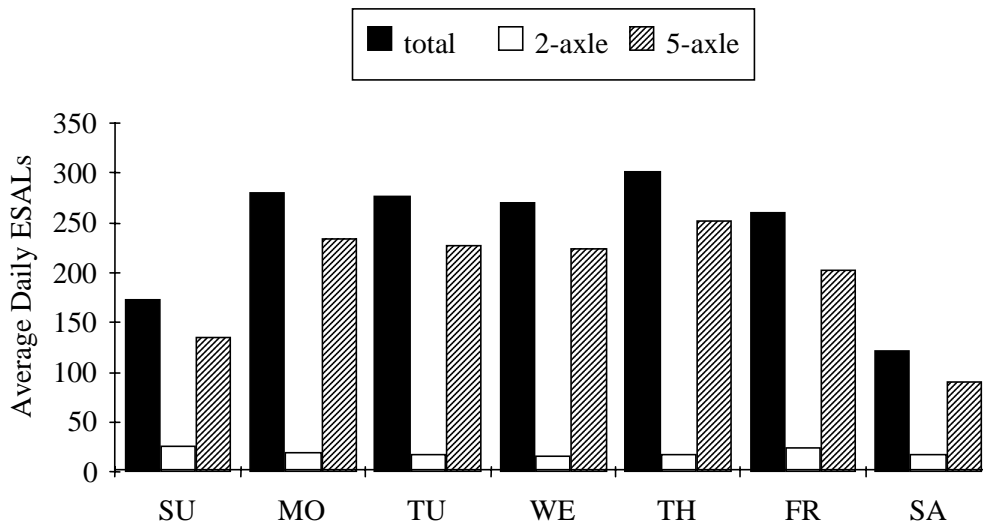


Figure 6.10 Average ESALs by Day of Week, North Site, Left Lane

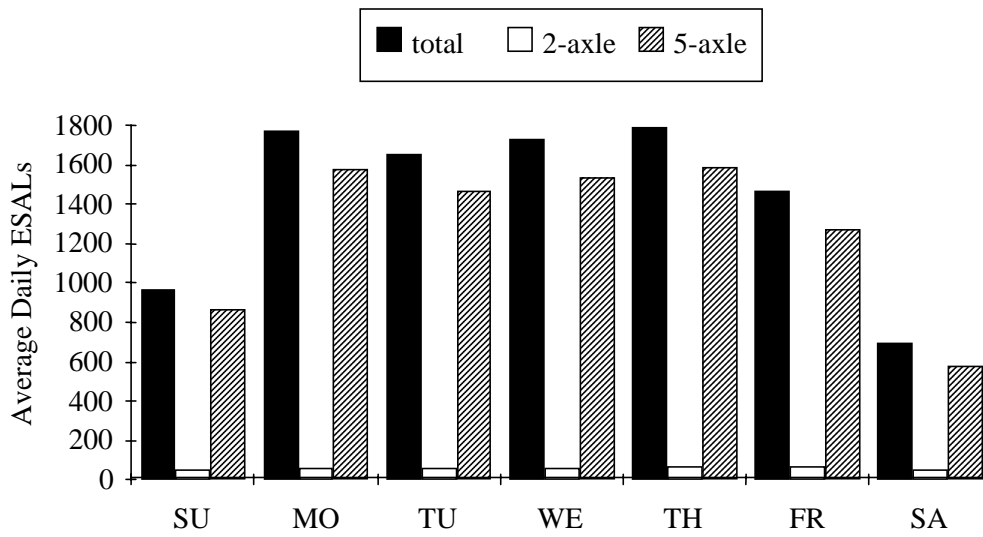


Figure 6.11 Average ESALs by Day of Week, South Site, Right Lane

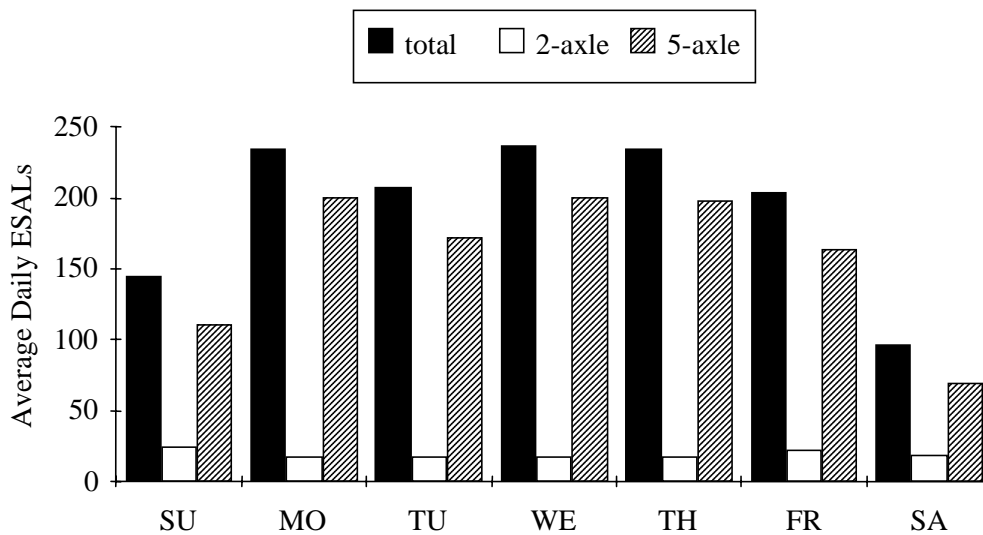


Figure 6.12 Average ESALs by Day of Week, South Site, Left Lane

Figures 6.13 through 6.16 show the average daily ESAL patterns by month for each location. At the north site, the average daily ESALs were highest in June in the right lane and September in the left lane. The low months were December in the right lane and January in the left lane. At the south site, the average daily ESALs were highest in July for both

lanes. The low months were December in the right lane and January in the left lane, the same as at the north site. In general, the summer months had higher ESALs and the winter months had lower ESALs. This seasonal variation may have been a result of trends in the logging industry or possibly of shipments bound for the Houston port.

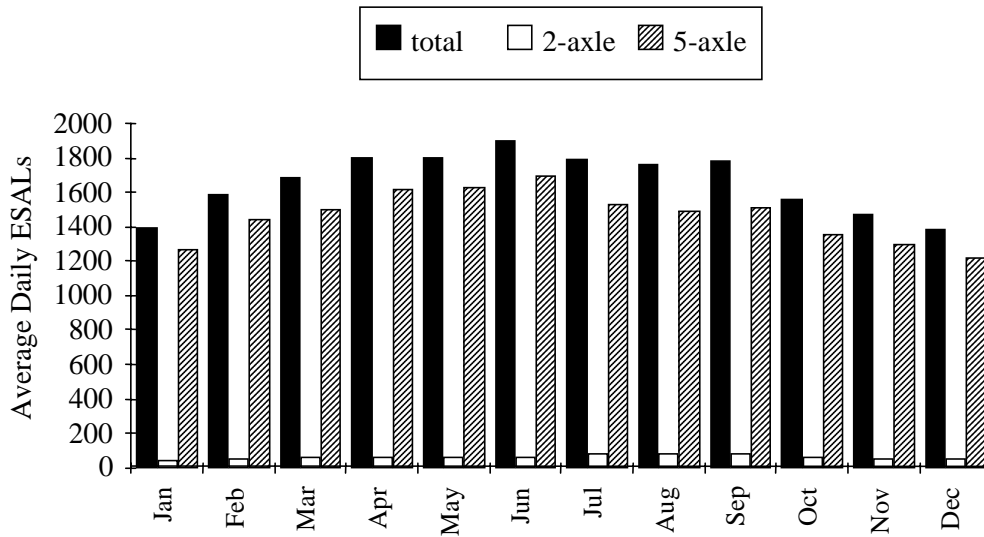


Figure 6.13 Average Daily ESALs by Month, North Site, Right Lane

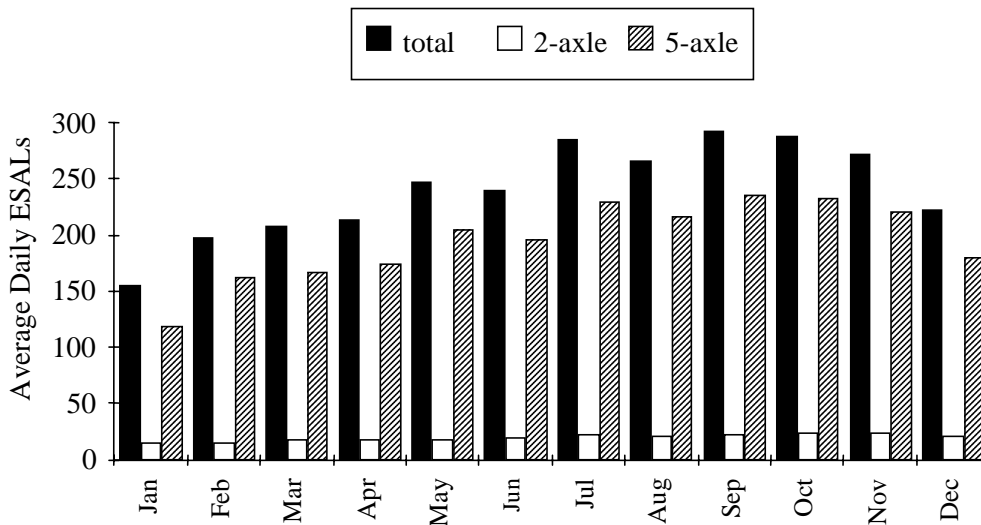


Figure 6.14 Average Daily ESALs by Month, North Site, Left Lane

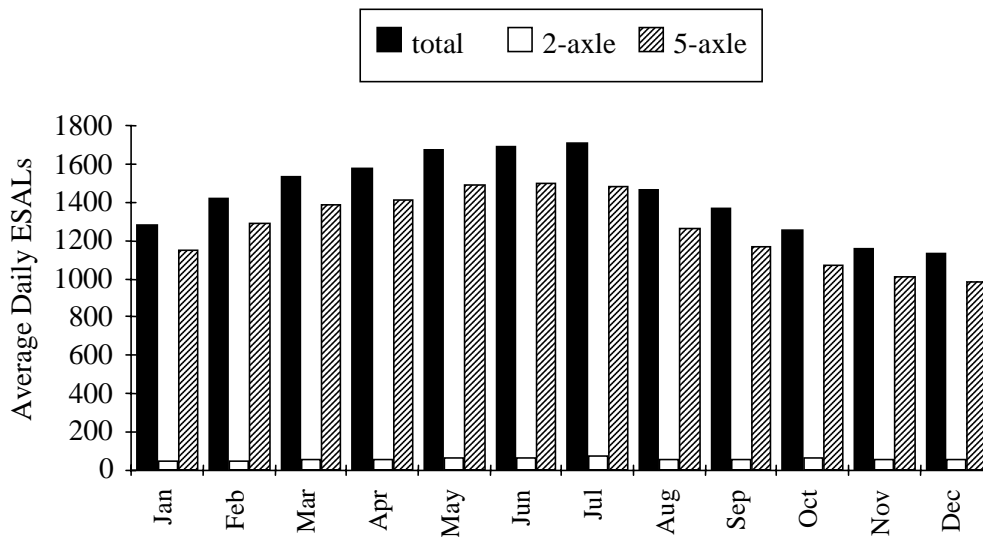


Figure 6.15 Average Daily ESALs, South Site, Right Lane

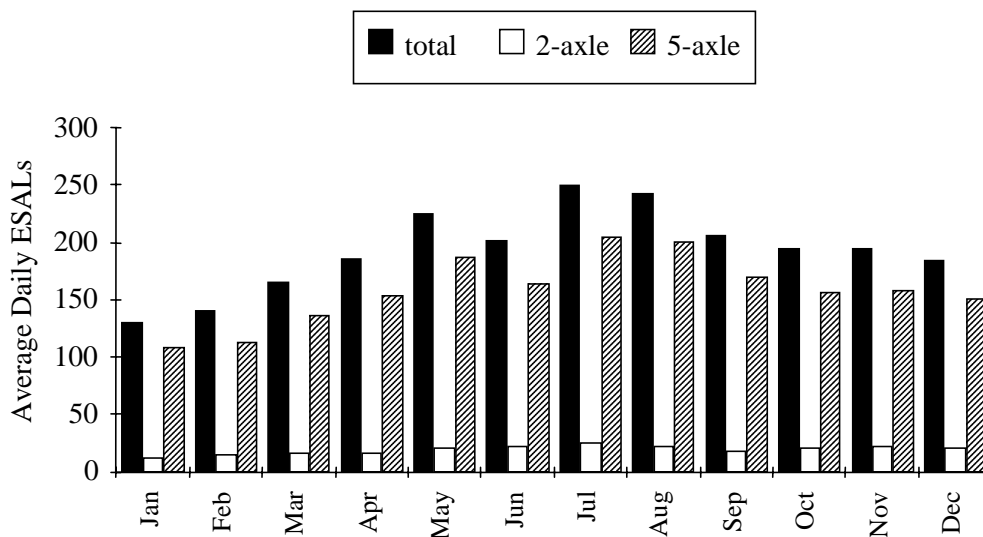


Figure 6.16 Average Daily ESALs by Month, South Site, Left Lane

In this section, daily and monthly trends of axle loads and ESALs were discussed. The right lane accounted for 84 percent of the total axle loads and 88 percent of the total ESALs. Axle loads and ESALs had lower values on weekends and during winter months and higher values on weekdays and during summer months. In the left lanes, two-axle vehicles accounted for a large proportion of the total axle loads — usually the majority of the axle

loads on weekends. ESALs contributed by two-axle vehicles in the left lane, though a higher proportion than in the right lane, were still a small part of the total ESALs.

6.3 Prediction Algorithm

A method that can be used to estimate ESALs from traffic volume counts will be discussed in this section. Permanent WIM equipment is relatively costly to install and operate, so temporary traffic volume counter/classifiers are commonly used to collect traffic data. If traffic volume data are available, sorted by vehicle class, the following method can be used to estimate the total ESALs along a route where the truck loading patterns are similar, but where traffic volume vary.

A method using five-axle vehicle volume as an example for estimating ESALs was developed from the traffic data collected on the Highway 59 Research Project (Minas 1994). This method can be expanded to include ESALs resulting from individual axle groups or to other vehicle classes.

Only five-axle vehicles, which contribute 92 percent of the total ESALs, were considered; data were from the right lane at the north site. ESALs per five-axle vehicle were calculated for each day of the year and the values separated into two seasons: one 5-month season (October through February), and one 7-month season (March through September). The average ESALs per five-axle vehicle for each day of the week are shown in Table 6.4. The average for the March through September season was 1.28 ESALs per five-axle vehicle, while the average for the October through February season was 1.04 ESALs per five-axle vehicle. Table 6.5 shows the percentage of total volume resulting from five-axle vehicles for each day of the week. Five-axle vehicles accounted for nearly 18 percent of the total traffic volume on Thursdays but only 7 percent on Saturdays.

Table 6.4 Average ESALs per Five-axle Vehicle for Each Day (Minas 1994)

	Mon	Tue	Wed	Thu	Fri	Sat	Sun
A) March–September							
Mean	1.35	1.31	1.31	1.30	1.28	1.16	1.25
St. dev	0.010	0.008	0.005	0.009	0.014	0.017	0.007
B) October–February							
Mean	1.11	1.05	1.05	1.02	1.04	0.94	1.07
St. dev	0.007	0.007	0.008	0.005	0.008	0.018	0.009

Table 6.5 Percentage of Five-axle Vehicles by Day of the Week

Mon	Tue	Wed	Thu	Fri	Sat	Sun	Total
17.09	16.46	17.60	17.73	15.07	6.96	9.10	100%

The following steps describe a method for estimating ESALs from volume counts, which include the number of five-axle vehicles for at least one 24-hour weekday period (AASHTO Guide 1986). If the number of 3S2 vehicles (three-axle tractor with two-axle semitrailer) is known then Step 1a can be used to estimate axle-group ESALs. A similar procedure may be used to estimate ESALs for axle groups of other vehicle classes.

Step 1 The number of five-axle vehicles should be multiplied by the appropriate average ESAL per vehicle factor depending on the month and day of the week from Table 6.4 to get the daily ESAL total.

Step 1a The number of drive tandems and trailer tandems for 3S2 vehicles should be multiplied by the average ESAL factors, such as those in Table 6.6; the axle-group ESALs should be added for the daily ESAL total.

Step 2 The daily ESAL total should be divided by the percentage of five-axle vehicles by day of week in Table 6.5 to get the weekly ESAL total; this should be multiplied by 52 to get the annual ESAL total.

Step 3 If the counts were taken for more than one 24-hour period, then the annual ESAL totals should be averaged.

Step 4 The total from Step 3 may be multiplied by a growth rate factor to obtain ESAL totals for future periods of time.

Step 5 The average annual ESAL totals should be divided by the five-axle vehicle class percentage (or 3S2 class percentage) to get the total annual average ESAL for each lane (e.g., 92 percent of total ESALs is a result of five-axle vehicles; about 80 percent is due to the 3S2 class).

Step 6 The total annual average ESAL should be multiplied by the lane distribution factor if there is more than one lane.

Step 7 The directional distribution factor should be used if necessary to calculate the ESALs for traffic in the opposite direction, assuming that the loading pattern is the same for trucks in both directions.

Tables 6.4 and 6.5 are derived from the traffic data collected in the right southbound lane of Highway 59 in 1993. Similar data should be collected from other locations in other years to check the validity of the values listed in the tables. A similar procedure may be used to calculate ESALs for other vehicle classes and these values should be added to the five-axle values for the total in Step 5, instead of multiplying by the vehicle-class percentage. If the volume counts also include vehicle classification by axle spacing, then axle-group statistics such as those in Figures 6.17 and 6.18 and in Table 6.6 can be used to determine the average loading for each axle group. The average ESAL per axle group for 3S2 vehicles for 12 March 1993 was 0.49 for the drive tandem, and 0.38 for the trailer tandem. The average ESALs for axle groups of other vehicle classes can be determined in a similar manner. In the above procedure, the daily ESAL total can be found by multiplying the axle groups by the appropriate factor and adding the axle-group ESALs to obtain the daily ESAL total.

Figure 6.17 shows the cumulative frequency distribution for axle-group loads of 3S2 vehicles at the north site in the right lane on 12 March 1993, while Figure 6.18 shows the cumulative frequency distribution for axle-group ESALs. Table 6.6 shows the axle-group

statistics for the same vehicles. Of the 898 five-axle vehicles, 776 (or 86 percent) were in the 3S2 class. Ten of the 3S2 vehicles, 1.3 percent, had steering axles over 5.4 Mg (12 kip), which accounted for 7.6 ESALs. The total of the ESALs for the 3S2 vehicles was 679, of which the steering axles contributed 1 percent, the drive tandems 56 percent, and the trailer tandems 43 percent. The top 5 percent of the axle groups contributed 19 percent of the ESAL share for drive tandems and 21 percent of the share for trailer tandems. The corresponding percentages for axle loads were 6 percent for the steering axles, 8 percent for drive tandems, and 9 percent for trailer tandems. In Figure 6.18, one outlying trailer tandem resulted in a jump for the last percentile from 3 ESALs to 4.7 ESALs. This demonstrates the disproportionate damage caused by overloaded axles. The steering axles were very consistent, while the tandem axles were considerably more variable, particularly at the upper end of the scale. The average of 0.88 ESALs per 3S2 vehicle was found by adding the average for each axle group. Calculations should be performed for other times of the year so that seasonal axle-group ESAL factors can be obtained.

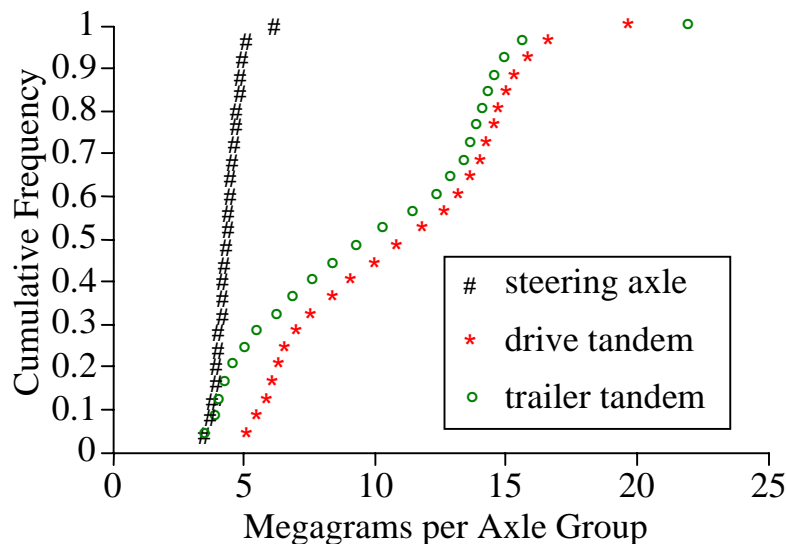


Figure 6.17 Cumulative Frequency Distribution for 3S2 Axle-group Loads, 12 March 1993, North Site, Right Lane
 1 kip = 0.4536 Mg

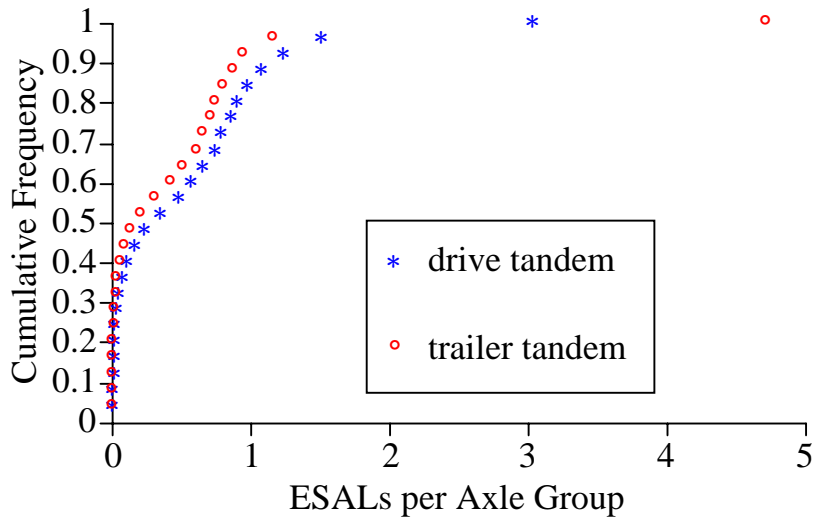


Figure 6.18 Cumulative Frequency Distribution for 3S2 Axle-group ESALs, 12 March 1993, North Site, Right Lane
 1 kip = 0.4536 Mg

Table 6.6 Axle Group Statistics for 3S2s, 12 March 1993, North Site, Right Lane
 1 kip = 0.4536 Mg

	Steering Axle	Drive Tandem		Trailer Tandem	
	Mg	Mg	ESAL	Mg	ESAL
Mean	4.5	11.0	0.49	9.7	0.38
St. Deviation	0.5	3.9	0.51	4.4	0.45
Minimum	1.6	4.1	0.004	2.6	0.0007
Maximum	6.4	19.8	3.05	22.0	4.72
95th Percentile	5.2	16.5	1.44	15.4	1.08

A method of estimating ESALs from traffic volume and class counts has been described in this section. If the traffic has been counted and classified for at least one 24-hour weekday period, then the ESALs for each axle group of each vehicle class can be estimated. A growth rate factor can be applied to forecast ESAL totals for future periods of time. To apply this method at other locations, a representative sample of WIM data would be

required to obtain the average ESAL factors for each axle group and vehicle class. It would be desirable if WIM data from a variety of locations and for different seasons could be collected so that a table of ESAL factors could be made available.

6.4 Summary

In Section 6.1, the formulas for calculating ESALs are described. The traffic data required are the axle loads for each vehicle and whether axles are single, tandem, or tridem. Steering axles heavier than 5.4 Mg (12 kip) require separate calculations. In Section 6.2, axle-load and ESAL trends were discussed. ESALs are higher on weekdays, during summer, and in the right lane. Most ESALs are due to five-axle vehicles. A method to estimate and forecast ESALs from traffic volume and class data is described in Section 6.3. ESALs can be obtained for each axle group of each vehicle class and growth factors may be applied to forecast ESAL totals.

Chapter 7 Lateral Position and Dual Tires

The lateral position of vehicle tires with respect to the edge of the lane is important because it can be used to describe the edge loading for slabs and the rutting pattern on asphalt pavements. Infrared sensors were used to calculate lateral position and also to indicate dual tires. The lateral position calculations and calibration were described in Chapter 4. The next section describes the lateral position patterns for the different classes of vehicles at each site and in each lane. Following this, the lateral position before and after moving the stripes at the north site is discussed. In the last section, the dual-tire data are discussed.

The infrared detector was located off the shoulder and the infrared source was on the pavement surface in the center of the lane, attached to the weighpad corner. The right- and left-lane calculations were different because of the differing shoulder widths, which caused the right-lane infrared receivers to be more distant from the infrared sources. There were four different calculations for lateral position, one for each lane at each site.

The formulas are as follows:

North site, right lane:	$LP = 8.5 - 0.00242VT$
North site, left lane	$LP = 8.7 - 0.00260VT$
South site, right lane	$LP = 8.6 - 0.00250VT$
South site, left lane	$LP = 9.2 - 0.00238VT$

LP = lateral position, feet

V = speed, miles per hour

T = infrared interrupt time, milliseconds

1 ft = 0.3048 m

1 mi/h = 1.609 km/h

7.1 Site and Lane Variation

In this section the lateral position data for each vehicle class are discussed, and the variations between lanes and between sites are described. Table 7.1 shows the average lateral position values for the different classes of vehicles for December 1993. At the north site, the

right-lane values were all higher than the left-lane values, while at the south site, the left-lane values were higher than the right-lane values, except for the five-axle vehicle class. The lateral position values indicate the distance of the outside front wheel from the outside lane edge. For the right lane, this would be the distance of the right front wheel from the right edge of the lane; for the left lane, this would be the distance of the left front wheel from the left edge of the lane. The lateral position generally decreased with increasing vehicle size, except in the case of the four-axle vehicles, which had a higher value than the three-axle vehicles. Many of the two-axle vehicles were single-unit trucks, and many of the three and four-axle vehicles were not trucks but rather passenger cars or pickups pulling one or two-axle trailers. Also, the six-axle vehicles in the left lanes had higher lateral position values than the five-axle vehicles; however, there were very few six-or-more axle vehicles in the left lanes, usually only one or two per day. Right-lane vehicles at the south site traveled closer to the shoulder than right-lane vehicles at the north site.

Table 7.1 Average Lateral Position Values for December 1993, meters

1 ft = 0.3048 m

	North		South	
	Right	Left	Right	Left
All Vehicles	1.20	0.81	0.88	1.06
2-axle, sp < 3.4	1.29	0.85	0.95	1.13
2-axle, sp > 3.4	1.15	0.82	0.84	1.03
3-axle	1.05	0.69	0.80	0.85
4-axle	1.08	0.73	0.80	0.92
5-axle	0.99	0.48	0.74	0.63
6-or-more axles	0.93	0.63	0.67	0.75

If all vehicles were to travel in the center of the lane, then the tires of trucks would travel closer to the lane edge than would passenger cars (because trucks are wider). At the north site, vehicles in the left lane traveled closer to the left shoulder than vehicles in the right lane traveled with respect to the right shoulder. Even though the left shoulder was quite a bit narrower than the right shoulder, vehicles in the left lane were more likely to be overtaking slower moving vehicles in the right lane and, thus, allowed more lateral clearance between vehicles. Vehicles in the right lane were more likely to be traveling without an overtaking

vehicle in the left lane. At the south site, only the five-axle vehicles traveled closer to the left-lane shoulder than to the right-lane shoulder. Owing to the traffic signal in Corrigan, a higher percentage of vehicles at the south site arrived simultaneously in both lanes. This may have accounted for the lower lateral position values in the right lane. At the south site, grass tended to grow higher and thicker than that at the north site, and in the summer months especially, the vegetation encroached on the shoulder. This may have accounted for the higher lateral position values in the left lane, because the left shoulder was only 1.2 m (4 ft) wide while the right shoulder was 3 m (10 ft) wide.

Figures 7.1 through 7.4 show the cumulative frequency distribution for lateral position at each location for 15 December 1993. Three- and four-axle vehicles are not shown for the left-lane figures because there were too few vehicles; six-axle vehicles are not shown for the same reason. Vehicles with a lateral position of 2 m (6.5 ft) or more were either traveling partially in the adjacent lane and, thus, missed the infrared light beam, or the infrared sensor may not have been working owing to grass covering the lens or some other reason. Grass was particularly a problem at the south site and in the left lane. The distribution of the three- and four-axle vehicles was very similar to the five-axle vehicles. In all cases, the two-axle vehicles traveled closer to the center of the lane.

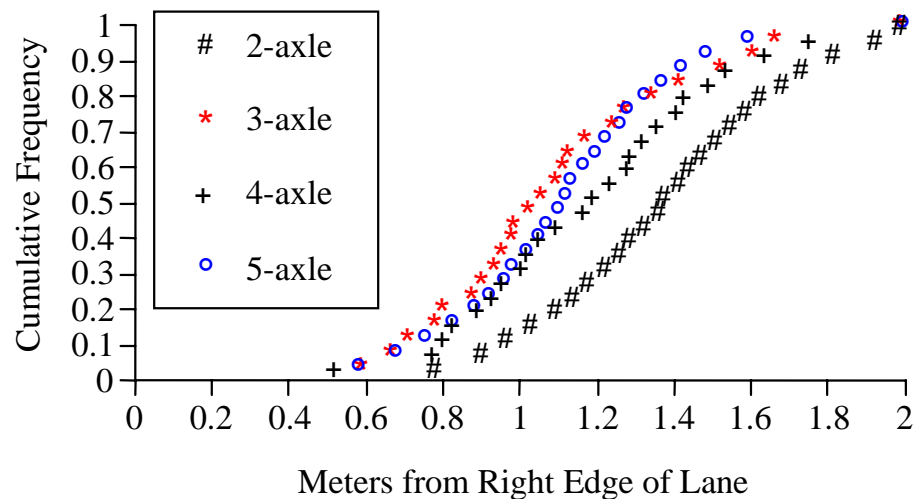


Figure 7.1 Lateral Position, North Site, Right Lane, 15 December 1993

1 ft = 0.3048 m

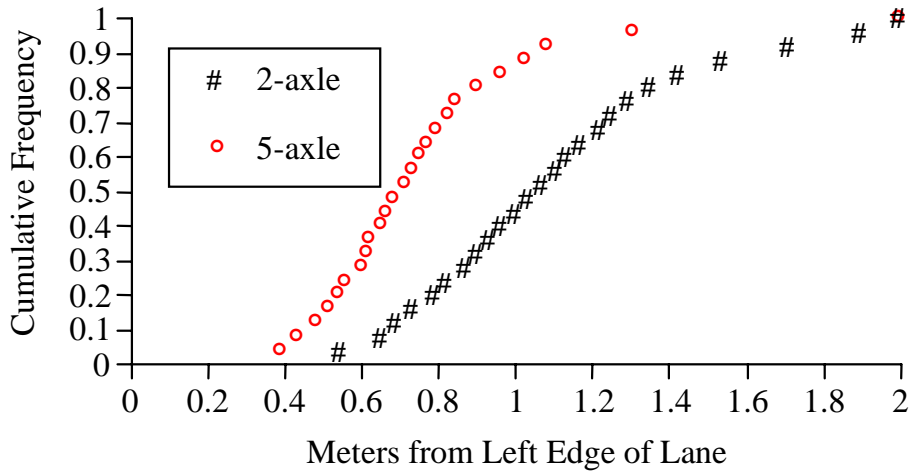


Figure 7.2 Lateral Position, North Site, Left Lane, 15 December 1993

1 ft = 0.3048 m

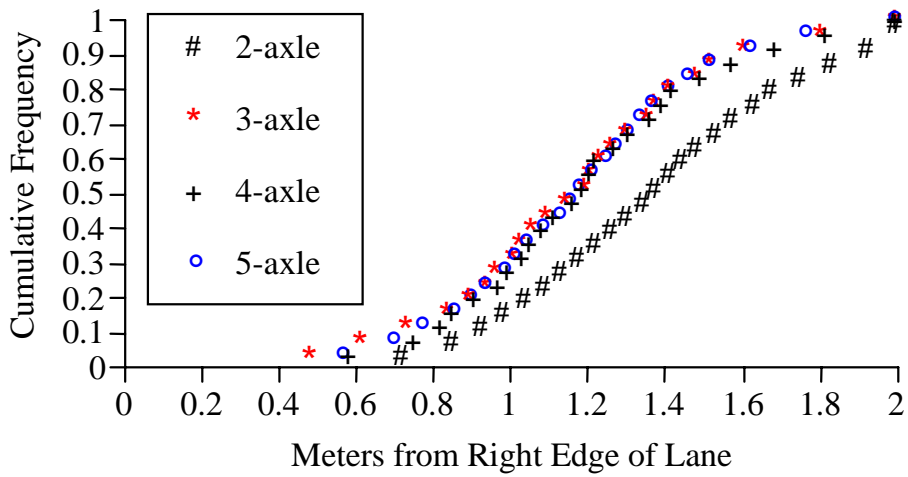


Figure 7.3 Lateral Position, South Site, Right Lane, 15 December 1993

1 ft = 0.3048 m

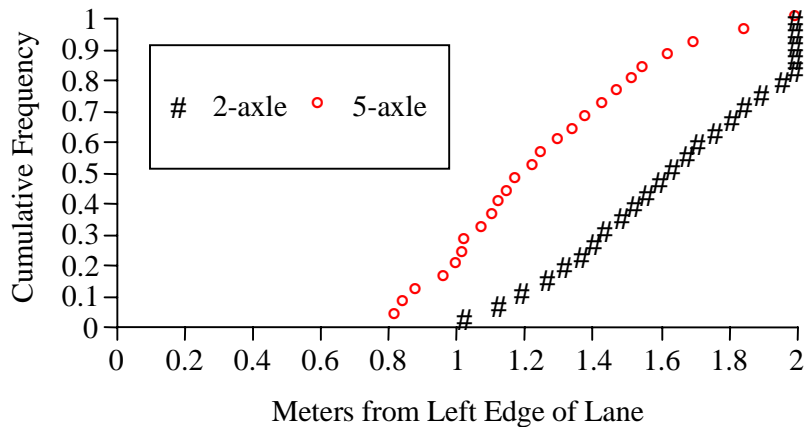


Figure 7.4 Lateral Position, South Site, Left Lane, 15 December 1993

1 ft = 0.3048 m

Vehicles with more axles traveled closer to the shoulder than vehicles with fewer axles. At the north site, the left-lane vehicles had smaller lateral position values, while at the south site, the right-lane vehicles had smaller lateral position values. Reasons for the differences may have been (1) overtaking vehicles in the left lane and (2) grass encroaching on the shoulders at the south site.

7.2 Stripe Moving

This section examines the lateral position data before and after moving the stripes at the north site. After construction, the longitudinal traffic stripes at the north site were painted in the wrong positions (too far to the left). The right ends of the weighpads in the right wheel paths were outside the paint stripes and the left shoulder became 0.9 m wide instead of 1.2 m (3 ft instead of 4 ft). The solid white line was off by 0.48 m (19 in.), the dashed white line was off by 0.25 m (10 in.), and the solid yellow line was off by 0.20 m (8 in.). These stripes were replaced between 15 and 22 April 1993. The incorrect traffic stripes are shown in Figure 7.5, and the correct traffic stripes are shown in Figure 7.6. Figures 7.7 and 7.8 show the lateral position of five-axle vehicles one month before and one month after the stripes were moved. The lateral position was measured from the edge of the weighpads, which was also the location of the stripes after the move. In Figure 7.7, the before-lane stripe would be at the 0.4 m (1.3 ft) mark while in Figure 7.8, the before-lane stripe would be at the -0.2 m

(-0.7 ft) mark. The five-axle vehicles in the left lane seem to have traveled farther to the left before the stripes were moved and farther to the right after the move, with the shift on the order of 0.2 m (0.7 ft), about the same distance the stripe was moved. The upper 20 percent of vehicles had about the same lateral position before and after. The five-axle vehicles in the right lane seem to have shifted on the order of 0.1 m (0.3 ft), but in the opposite direction from the stripe move.

Several months of lateral position data were collected before the pavement stripes at the north site were shifted to the proper location. In the left lane, five-axle vehicles seemed to shift lateral position about the same amount that the stripe was shifted. However, the right-lane vehicles did not seem to shift lateral position, at least not in the expected direction.

7.3 Dual-Tire Data

This section discusses how infrared sensors can measure tire size and indicate dual tires. Some dual-tire statistics are tabulated and the differences between vehicle classes discussed.

Infrared sensors have been used previously to measure tire size. A set of three infrared sensors were used to measure the tire-contact length and projected contact length in the summer of 1990 on Interstate 35 near Jarrell, Texas, in an effort to estimate the tire-contact area and to correlate the tire-contact area with wheel loads determined by WIM (Garner, Lee, and Huang 1990). Two infrared light beams were perpendicular to the direction of travel and measured the vehicle speed and the length of tires. A third infrared sensor was at an angle and was used to measure the projected tire length. Each infrared light beam was just above the pavement surface. The presence of dual tires could be determined from comparison of the length and projected length of the tires. A study was conducted for the Oklahoma Turnpike Authority (OTA) in August 1990 on Interstate 44 near Oklahoma City to determine the feasibility of using infrared sensors to audit toll collection. The criteria used by the OTA for sorting vehicles into different classes for toll collection purposes are the number of axles per vehicle and whether tires are single or dual. An infrared light beam slightly above the pavement surface and at a 60° angle to the direction of travel was used to indicate whether tires were single or dual. The dual-tire calculations were discussed in Chapter 4. Front-axle tires are assumed to always be single. The infrared light beam

interrupt times for each succeeding tire are compared to the interrupt time for the first tire of each vehicle. If the interrupt time is more than 20 percent greater than the time for the front tire, the succeeding tire is defined as dual. Trucks with tires of various sizes were observed and the 20 percent value was found to be sufficient.

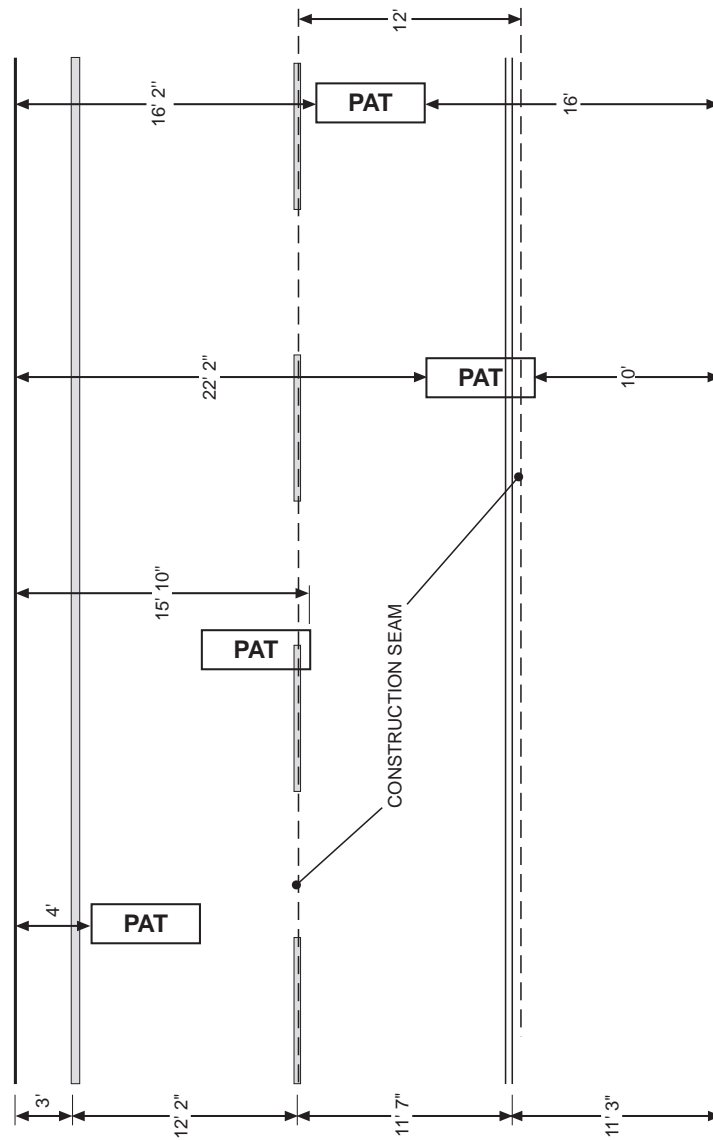


Figure 7.5 Incorrect Location of Traffic Stripes

1" = 25.4 mm

1' = 0.3048 m

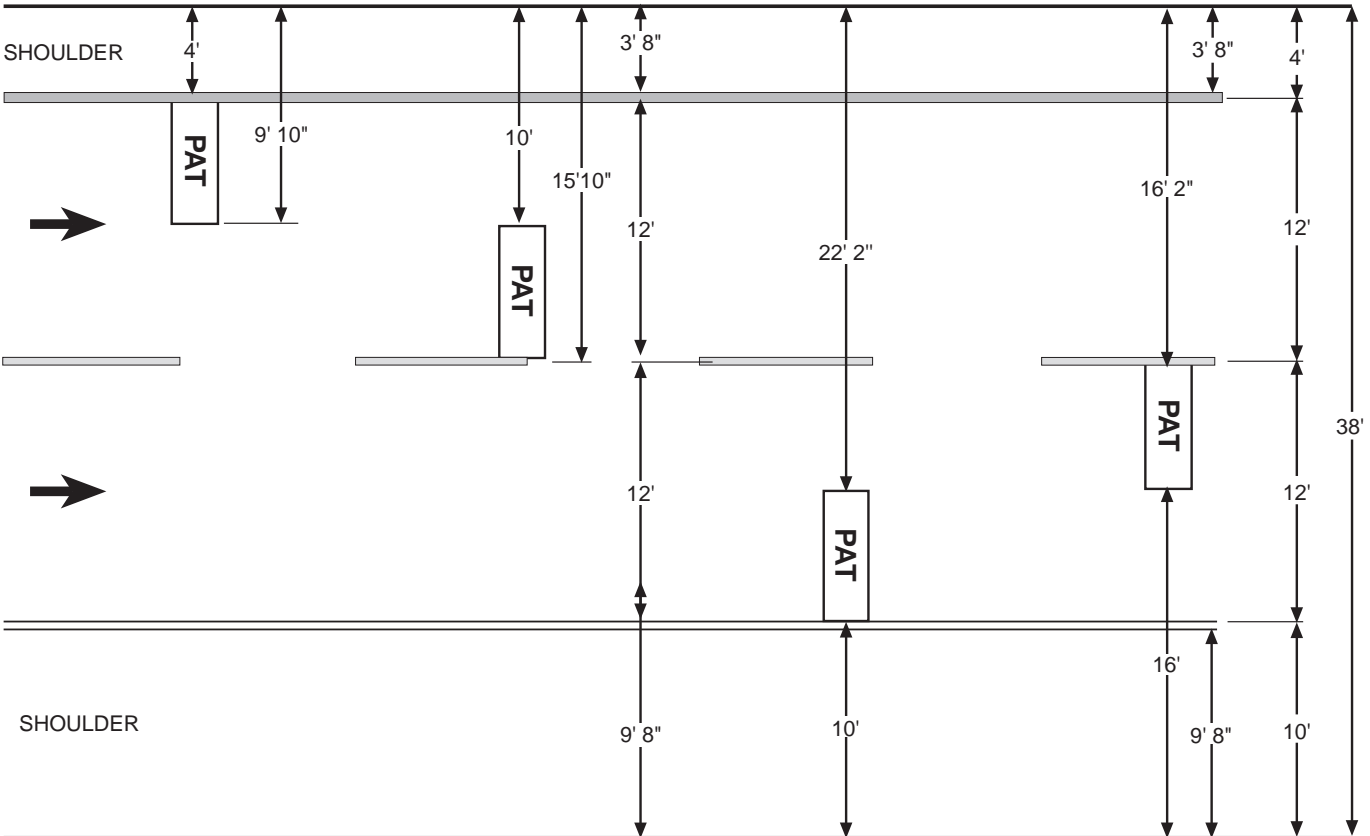


Figure 7.6 Correct Location of Traffic Stripes

1" = 25.4 mm 1' = 0.3048 m

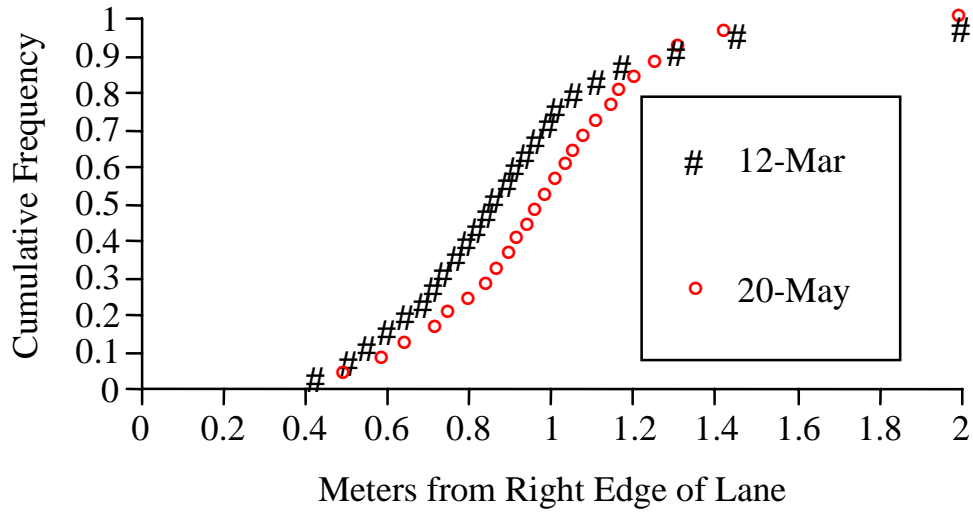


Figure 7.7 Lateral Position of Five-axle Vehicles, Right Lane

1 ft = 0.3048 m

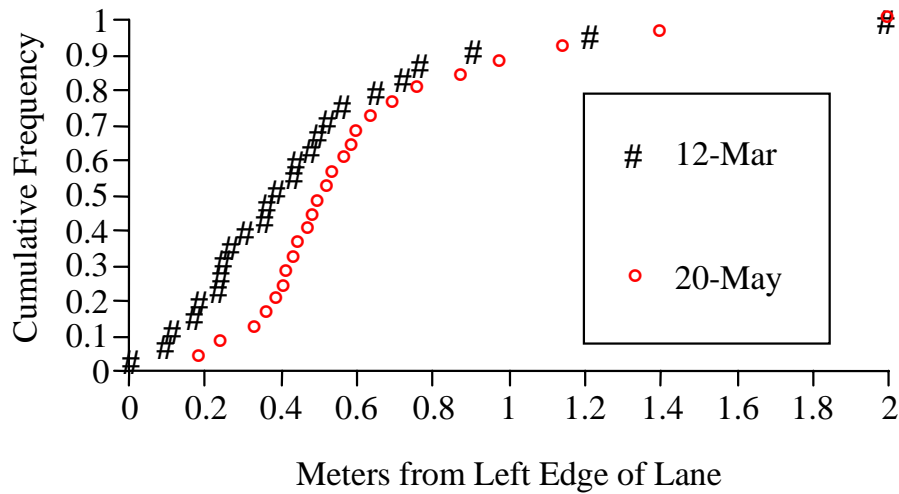


Figure 7.8 Lateral Position of Five-axle Vehicles, Left Lane

1 ft = 0.3048 m

Table 7.2 shows the proportions of vehicles with dual tires for vehicles having three or more axles for 1993. Many days were missing infrared data, especially at the south site, so the actual figures should be higher. Table 7.3 shows the dual-tire data for the month of December 1993. The two-axle vehicle class was subdivided by an axle spacing of 3.4 m (11

ft). The shorter vehicles were between 67 percent and 76 percent of all two-axle vehicles. It is difficult to compare lanes and sites because the infrared sensors were out of service on a number of occasions because of grass blocking the light beams and the difficulty of maintaining precise alignment. Even if the infrared sensors were operating all the time, many vehicles traveling partially in the adjacent lane would not interrupt the light beams and would have interrupt times of zero. Vehicles with zero interrupt times were not distinguished from those vehicles that had nonzero interrupt times but had only single tires. Therefore, all the percentages listed in the following tables are low. The five- and six-axle classes should have nearly 100 percent dual tires. The three- and four-axle classes, which include passenger cars or pickups pulling trailers, should have around 75 percent dual tires. The two-axle class should have around 10 percent dual tires. The right-lane infrared sensor at the north site seems to have been the most reliable because the proportions for each vehicle class are higher compared to the other infrared sensors.

Table 7.2 Proportion of Vehicles with Dual Tires, 1993

	North		South	
	Right	Left	Right	Left
3-axle	58%	51%	36%	32%
4-axle	62%	49%	38%	26%
5-axle	94%	90%	62%	57%
6-or-more axle	92%	83%	64%	51%

Table 7.3 Proportion of Vehicles with Dual Tires, December 1993

	North		South	
	Right	Left	Right	Left
All Vehicles	25%	14%	21%	12%
2-axle, sp < 3.4	3%	6%	4%	3%
2-axle, sp > 3.4	18%	10%	16%	10%
2-axle (all)	6%	7%	7%	5%
3-axle	63%	53%	47%	54%
4-axle	61%	46%	45%	38%
5-axle	98%	95%	75%	96%
6-or-more axle	96%	81%	78%	77%

This chapter has discussed the traffic data collected with infrared sensors on the Highway 59 Research Project. The lateral position data showed that large vehicles traveled closer to the shoulder than small vehicles. Left-lane vehicles tended to travel closer to the shoulder at the north site, while right-lane vehicles traveled closer at the south site. The stripe moving data at the north site showed that the left-lane vehicles shifted with the stripe, while the right-lane vehicles did not shift with the stripe. The proportion of large vehicles with dual tires was more than for small vehicles, but comparing dual tires between lanes and between sites is difficult because many days had missing infrared data.

More work needs to be done with the infrared data to sort out vehicles that do not interrupt the light beam, and to distinguish the vehicles passing on days or at times when the infrared sensors are not operating. The lateral position data may be used with the weighpad data to adjust for vehicles that only cross one weighpad. The dual-tire data may be used as an additional criterion for sorting vehicle classes.

Chapter 8 Temperature

Temperature data are important for pavement design because the behavior and properties of materials are temperature dependent. Hot temperatures can lead to rutting of asphalt pavements, while cold temperatures can lead to cracking. The pavement temperature can be significantly hotter than the air temperature, especially during the summer. For this study, hourly air and pavement temperature data were collected at each location.

8.1 Installation and Calibration

Thermocouples for air and pavement temperature were added to each WIM system and calibrated on 25 January at the south site and 8 February 1993 at the north site. A new erasable programmable read-only memory (EPROM) installed in April at the north site and in May at the south site enabled the temperature data to be saved once every hour and downloaded. The air thermocouples were suspended outside each cabinet on the north side so they would tend to be in the shade more often. Sawcuts were made in the right shoulders about halfway across to the lane edge, and the pavement thermocouples were buried under a layer of caulk approximately 13 mm (0.5 in.) deep. The calibration apparatus consisted of a container of ice water and a thermometer heated over a butane stove to a temperature as high as 57°C (136°F). The output from the thermocouples was observed by means of a laptop computer. Each thermocouple at each site had different calibration formulas. The highest temperatures observed were 57°C (136°F) for the pavement and 50°C (122°F) for the air, both in July 1993. The lowest temperatures observed were -3°C (26°F) for the air and 3°C (38°F) for the pavement, both in November 1993. The summer temperatures were generally higher at the south site than at the north site.

The calibration data were plotted on graph paper and appeared to be quite linear, so the least-squares method was used to calculate the formulas. The following formulas were used to convert the thermocouple readings (X) to temperature (T) in °F.

$$\text{North site, air: } T = -429 + 0.216X$$

$$\text{North site, pavement: } T = -443 + 0.217X$$

$$\text{South site, air: } T = -412 + 0.209X$$

$$\text{South site, pavement: } T = -490 + 0.246X$$

$$^{\circ}\text{F} = 32 + 1.8^{\circ}\text{C}$$

The daily high and low temperatures for Livingston, about 40 km (25 mi) south of the sites, are listed in “National Climatological Data, Texas,” 1993. After checking these data, it was confirmed that the calibrated temperatures were within a reasonable range.

8.2 Daily and Seasonal Trends

Figures 8.1 and 8.2 show the average daily temperature extremes at the north and south sites for the air and pavement thermocouples. The months of April through December 1993 were measured at the north site, and May through December 1993 were measured at the south site. The pavement temperatures were higher than the air temperatures except for November and December at the north site, when the maximum air temperatures were slightly higher than the pavement temperatures.

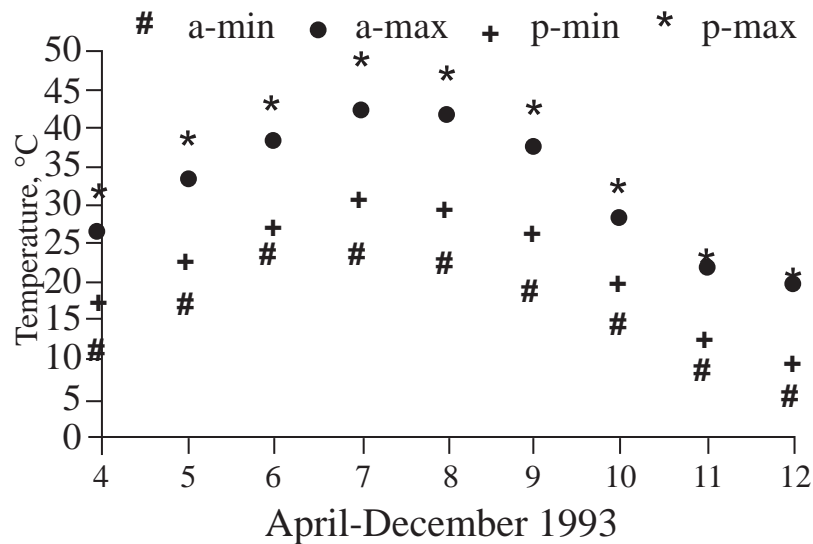


Figure 8.1 Average Daily Temperature Extremes, North Site

$$^{\circ}\text{F} = 32 + 1.8^{\circ}\text{C}$$

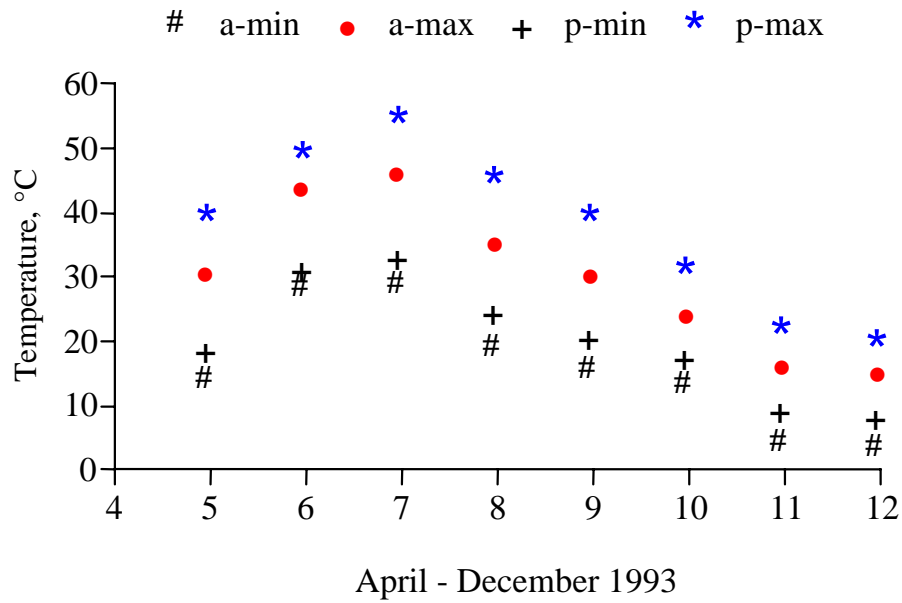


Figure 8.2 Average Daily Temperature Extremes, South Site

$$^{\circ}\text{F} = 32 + 1.8^{\circ}\text{C}$$

Figures 8.3 through 8.10 show the hourly temperature for each site for selected days in May, July, October, and December. The patterns for May and July were quite similar, with the pavement temperatures always higher than the air temperatures except for several hours in the mornings. The morning lows and afternoon highs occurred about three hours later for the pavement than for the air. The pavement temperature trends were fairly smooth while the air temperature curves were more irregular. The patterns for October and December were similar, with the pavement temperature trends close to linear. The differences between the air and pavement temperatures were in the range of 3°C (5°F), while the differences between the air and pavement temperatures for May and July were in the range of 11°C (20°F).

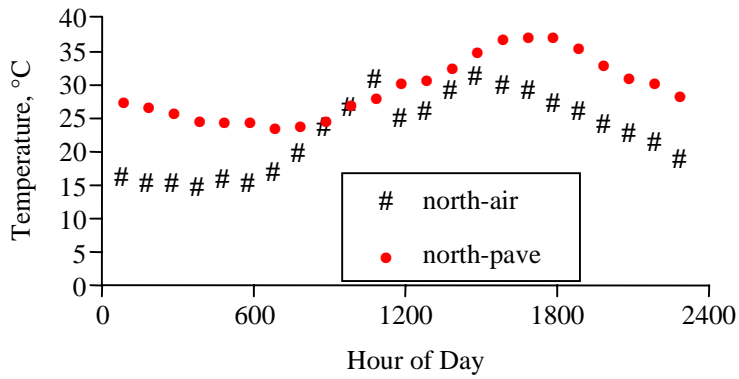


Figure 8.3 Hourly Temperature, 21 May 1993, North Site
 $^{\circ}\text{F} = 32 + 1.8^{\circ}\text{C}$

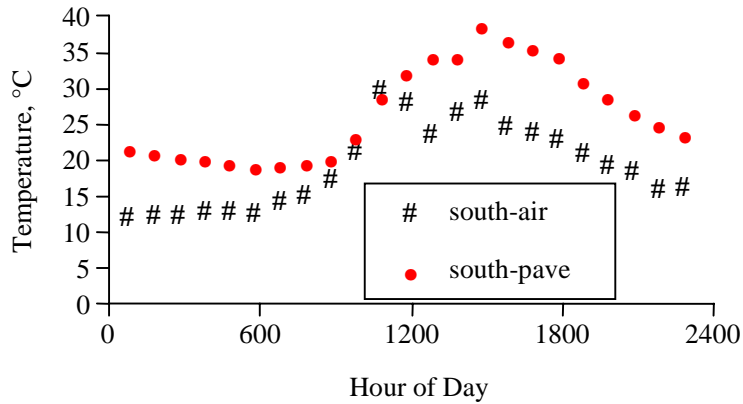


Figure 8.4 Hourly Temperature, 21 May 1993, South Site
 $^{\circ}\text{F} = 32 + 1.8^{\circ}\text{C}$

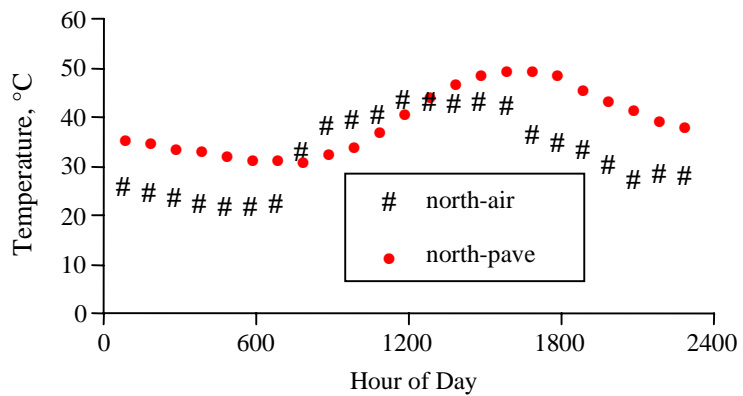


Figure 8.5 Hourly Temperature, 23 July 1993, North Site
 $^{\circ}\text{F} = 32 + 1.8^{\circ}\text{C}$

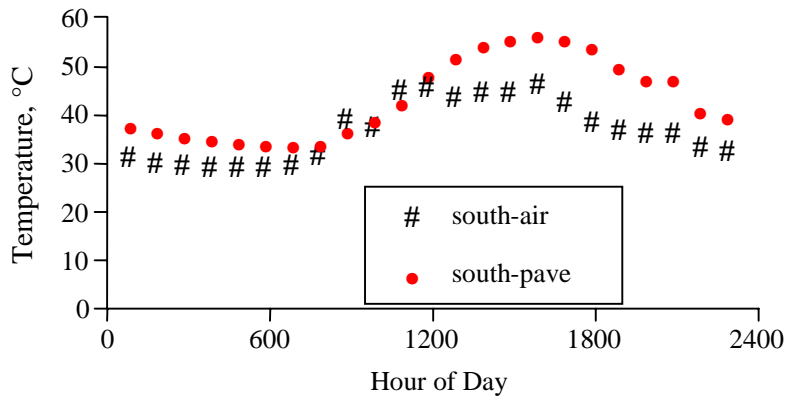


Figure 8.6 Hourly Temperature, 23 July 1993, South Site
 $^{\circ}\text{F} = 32 + 1.8^{\circ}\text{C}$

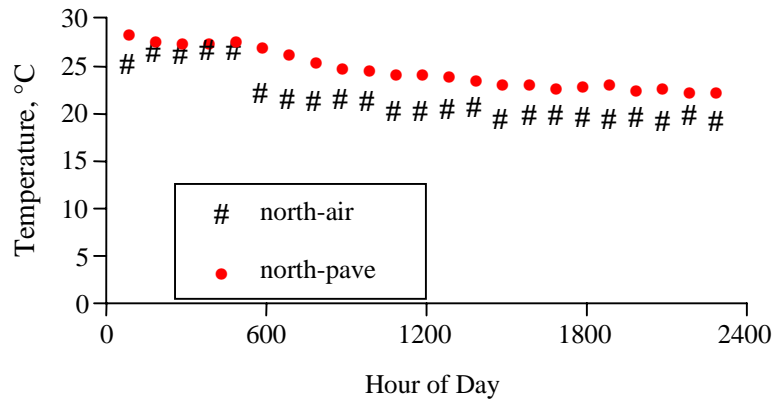


Figure 8.7 Hourly Temperature, 20 October 1993, North Site
 $^{\circ}\text{F} = 32 + 1.8^{\circ}\text{C}$

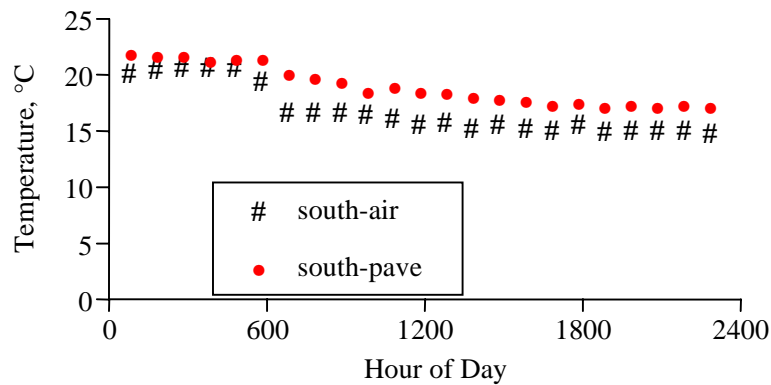


Figure 8.8 Hourly Temperature, 20 October 1993, South Site
 $^{\circ}\text{F} = 32 + 1.8^{\circ}\text{C}$

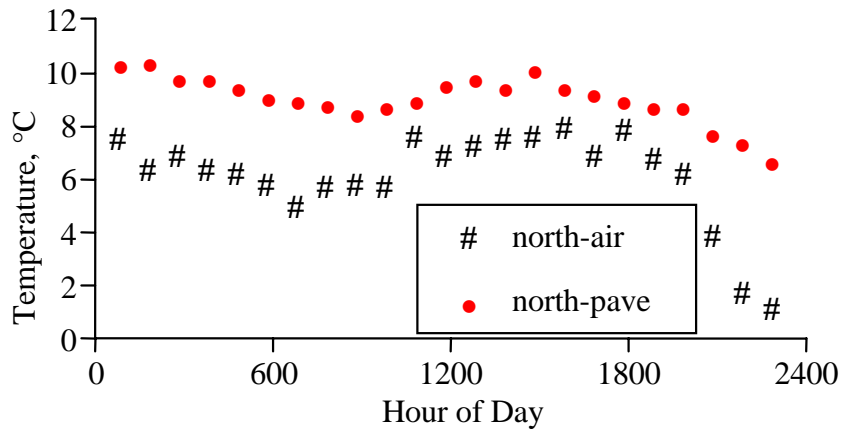


Figure 8.9 Hourly Temperature, 22 December 1993, North Site
 $^{\circ}\text{F} = 32 + 1.8^{\circ}\text{C}$

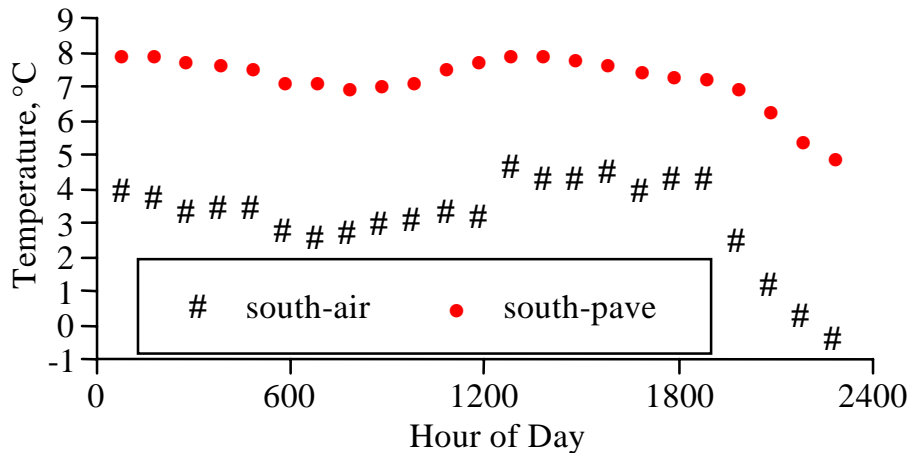


Figure 8.10 Hourly Temperature, 22 December 1993, South Site
 $^{\circ}\text{F} = 32 + 1.8^{\circ}\text{C}$

Temperature data help to describe the behavior and properties of pavement materials. Thermocouples were added to each WIM system on the Highway 59 Research Project to collect both air and pavement temperature. The maximum temperatures were recorded in the pavements in July, while the minimum temperatures were recorded by the air thermocouples in November. Hourly pavement temperatures for selected days are shown. Except for a few hours in the mornings, the pavement temperatures were always higher than the air temperatures. The difference between pavement and air temperature was greater during the summer than during the winter.

Chapter 9 Conclusion

The primary cause of damage to highway pavements is traffic loading. The AASHO Road Test was discussed in Chapter 2. The road test demonstrated that the damage resulting from axle loads is nonlinear with an approximately fourth-power relationship, thus doubling the axle load results in multiplying the pavement damage by 16. Only uniform axle loads were applied at the road test, so the equivalent single axle load (ESAL) concept was introduced to describe the damage caused by mixed traffic loads in terms of a standard axle load. The number of applications of a standard, e.g., 8.2 Mg (18-kip), single (dual-tire) axle load that will cause the same damage to a given pavement structure as one application of a given axle load on a defined axle type is called an ESAL factor. The cumulative number of ESALs observed or estimated within a defined time period are referred to as ESALs.

The construction of two pavement test sections in the southbound lanes of Highway 59 and the installation of augmented weigh-in-motion (WIM) systems to measure traffic loads were discussed in Chapter 3. The traffic data collected by the WIM systems include number of vehicles, wheel loads, speed, number of axles, axle spacing, lateral position, and indication of single or dual tires. The WIM systems were installed in 1992, with continuous data collection beginning in December 1992. Bending-plate weighpads manufactured by PAT collect wheel load and other traffic data. Infrared sensors collect lateral position and dual-tire data. Thermocouples collect air and pavement temperature. The main problems experienced with the infrared sensors were bolts shearing off the source housings under traffic, moisture shorting out the electrical connections, and grass growing in front of the detectors on the shoulder. After shear pins were added to the source housings, and epoxy splicing kits were used for the electrical connections, the first two problems were mostly resolved.

The data analysis and calibration of the WIM system were discussed in Chapter 4. The PAT software calculates weight, speed, and axle spacing for each vehicle on-site. A modem may be used to download data files over telephone lines. The first modems used were not suited to the temperature extremes in the roadside cabinet, which necessitated frequent trips to download data directly to a laptop computer. Later modems were more robust and reliable. An Excel macro was used to sort vehicles into different files by vehicle class, to calculate ESALs and lateral position for each vehicle, and to summarize the data for

each lane and vehicle class. At first, the Excel macro was very time consuming, but later versions and faster computers helped to increase the data-processing rate.

Volume, speed, axle load, and ESAL data were discussed in Chapters 5 and 6. An average of 7,000 vehicles passed each day in the southbound lanes in 1993. The average speeds ranged from 98 km/h to 115 km/h (62 mi/h to 72 mi/h), depending on the vehicle class and location. Right-lane vehicles accounted for 75 percent of the total volume, 84 percent of the total axle loads, and 88 percent of the total ESALs. Two-axle vehicles made up 75 percent of the right-lane vehicles and 90 percent of the left lane vehicles. There was a higher proportion of two-axle vehicles on the weekends. The two highest traffic volume days of the year were the Sundays following the Thanksgiving and Christmas holidays. The majority of ESALs, especially in the right lane, were contributed by five-axle vehicles. Higher ESALs occurred on weekdays and during the summer months.

A method that can be used to estimate ESALs from traffic volume counts is discussed in Chapter 6. The average ESAL per axle-group of a given vehicle class is used as a factor to convert vehicles per day to ESALs per day. The ESAL factor may depend on the day of the week or the season of the year. A growth rate factor may be applied to obtain ESAL totals for future periods of time. ESALs may be estimated for each axle-group of each vehicle class. Sample 3S2 data were used to calculate the average ESAL factors for the drive tandem and trailer tandem. To apply this method at other locations, a representative sample of WIM data would be required to obtain the ESAL factors. It would be desirable if WIM data from a variety of locations and for different seasons could be collected so that a table of ESAL factors could be made available.

The lateral position data discussed in Chapter 7 showed that left-lane vehicles at the north site and right-lane vehicles at the south site tended to travel closer to their respective shoulders. Vehicles with more axles tended to travel closer to the shoulders than vehicles with fewer axles. Vehicles with more axles were also more likely to have dual tires. More work needs to be done with the infrared data to sort out vehicles that do not interrupt the light beam, and to distinguish the vehicles passing on days or at times when the infrared sensors are not operating. The lateral position data may be used with the weighpad data to adjust for vehicles that cross only one weighpad.

The temperature data discussed in Chapter 8 showed that the pavement temperature was almost always higher than the air temperature except for a few hours in the mornings and on some days in the winter months. The highest observed temperatures were 57°C (136°F) for the pavement and 50°C (122°F) for the air in July. The lowest temperatures observed were 3°C (38°F) for the pavement and -3°C (26°F) for the air in November. The summer temperatures at the south site were generally higher than those at the north site.

This portion of Research Project 7-987 provided an opportunity to collect and analyze continuous, mixed-traffic data for correlation with concurrently measured performance of rigid and flexible pavement test sections. A unique WIM system measured not only wheel loads, speed, and axle spacing, but also lateral position of tires, single or dual tires, and air and pavement temperatures. An Excel spreadsheet macro was written to display, arrange, and summarize a massive amount of data each day. Data were analyzed for one year to establish daily, weekly, and monthly patterns. Traffic loading data are essential to plan and design adequate, cost-effective highway pavements.

References

- Highway Research Board. "The AASHO Road Test: History and Description of Project." Highway Research Board, Special Report 61A, 1961.
- Highway Research Board. "The AASHO Road Test Report 5: Pavement Research." Highway Research Board, Special Report 61E, 1962.
- American Association of State Highway and Transportation Officials. "AASHTO Guide for Design of Pavement Structures." American Association of State Highway and Transportation Officials (AASHTO), Washington, D.C., 1986.
- American Association of State Highway and Transportation Officials. AASHTO Guide for Design of Pavement Structures (2nd edition). AASHTO, Washington, D.C., 1993.
- American Association of State Highway and Transportation Officials. AASHTO Guide for Design of Pavement Structures, Volume 2, Appendix MM, Extension of Equivalency Factor Tables, AASHTO, Washington, D.C., 1988.
- Carey, W. N., Jr., and P. E. Irick. "Relationships of AASHO Road Test Pavement Performance to Design and Load Factors." *The AASHO Road Test Conference Proceedings*, Highway Research Board, Special Report 73, 1962.
- Cho, Yoon-Ho, and B. Frank McCullough. "Initial Performance of Asphalt Overlays on Jointed Concrete Overlay (JCP) in Field Test Sections in Lufkin, Texas." Research Report 987-4, Center for Transportation Research, The University of Texas at Austin, 1995.
- Cunagin, Wiley D. "Use of Weigh-in-Motion Systems for Data Collection and Enforcement." NCHRP Synthesis of Highway Practice 124, Transportation Research Board (TRB), Washington, D.C., 1986.

DAW100 Specifications. Pietzsch Automatisierungstechnik GmbH, PAT Traffic Control Corporation, 1665 Orchard Drive, Chambersburg, PA 17201, Telephone: (717) 263-7655, FAX: (717) 263-7845.

Garner, Joseph E., Clyde E. Lee, and Liren Huang. "Infrared Sensors for Counting, Classifying, and Weighing Vehicles." Research Report 1162-1F, Center for Transportation Research, The University of Texas at Austin, 1990.

Garner, Joseph E., Clyde E. Lee, and Liren Huang. "Photoelectric Sensors for Counting and Classifying Vehicles." *Transportation Research Record 1311*, TRB, Washington, D.C., 1991.

Garner, Joseph E., and Clyde E. Lee. "Augmented Weigh-in-Motion System for Traffic Data Collection and Analysis." *Transportation Research Record 1501*, TRB, Washington, D.C., 1995.

Huang, Yang H. *Pavement Analysis and Design*. Prentice Hall, Englewood Cliffs, NJ, 1993.

Kell, James H., and Iris J. Fullerton. *Traffic Detector Handbook*. Institute of Transportation Engineers, Washington, D.C., 1991.

Lee, Clyde E., P. R. Shankar, and Bahman Izadmehr. "Lateral Placement of Trucks in Highway Lanes." Research Report 310-1F, Center for Transportation Research, The University of Texas at Austin, 1983.

Lee, Clyde E., and Jeffrey W. Pangburn. "Preliminary Research Findings on Traffic-Load Forecasting Using Weigh-in-Motion Data." Research Report 987-5, Center for Transportation Research, The University of Texas at Austin, 1996.

Leidy, Joseph Paul, Clyde E. Lee, and Robert Harrison. "Measurement and Analysis of Traffic Loads across the Texas-Mexico Border." Research Report 1319-1, Center for Transportation Research, The University of Texas at Austin, 1995.

Minas, Yohannes. "Weigh-in-Motion and Infrared Detector Systems for Traffic Load Forecasting." Master's thesis, The University of Texas at Austin, 1994.

National Climatological Data, Texas. Vol. 98, National Climatic Center, National Oceanic and Atmospheric Administration, Asheville, NC, 1993.

Opcon Industrial Sensors Catalog. Opcon, Inc., Everett, WA, 1990.

Qu, Tongbin, Clyde E. Lee, and Liren Huang. "Traffic-Load Forecasting Using Weigh-in-Motion Data." Research Report 987-6, Center For Transportation Research, The University of Texas at Austin, 1996.

American Society for Testing and Materials. "Standard Specification for Highway Weigh-in-Motion (WIM) Systems with User Requirements and Test Method, Designation: E 1318-94." *1996 Annual Book of ASTM Standards*, Vol. 04.03, American Society for Testing and Materials, West Conshohocken, PA, 1996.

Federal Highway Administration. *Traffic Monitoring Guide* (3rd edition). Federal Highway Administration, Office of Highway Information Management, 1995.

